Computer Aided Interventions and Medical Robotics

Image-Guided Procedures: A Review

Ziv Yaniv and Kevin Cleary

Technical Report
CAIMR TR-2006-3

April 2006

Georgetown University,
Imaging Science and Information Systems Center,
Washington, DC, 20007,
http://www.caimr.georgetown.edu/

Image-Guided Procedures: A Review

Ziv Yaniv and Kevin Cleary

Imaging Science and Information Systems Center,
Department of Radiology, Georgetown University Medical Center,
Washington, DC, USA.
Email:{zivy,cleary}@isis.georgetown.edu

April 2006

Abstract

This paper reviews the current state of the art in Image-Guided Procedures (IGP), focusing on key enabling technologies, and image-guided systems. Based on an idealized time-line view of medical procedures (pre-procedure, during the procedure, and post procedure), we identify the following key technologies associated with the different procedure steps: (1) medical imaging and image processing; (2) data visualization; (3) segmentation; (4) registration; (5) tracking systems; and (6) human computer interaction. We discuss these technologies as they pertain to IGP, and describe image guidance systems from several medical disciplines through their use of these building blocks. From this survey we note that current image-guided systems assume rigid or nearly rigid anatomical structures, thus limiting their use. Finally, we present current and future directions of research aimed at image guidance for deformable anatomical structures.

1 Introduction

Motivated by better results and lower overall costs, clinical practice is rapidly replacing traditional open surgical procedures with minimally invasive techniques. Most notably, this is a transition from direct visual feedback to indirect, image-based feedback.

This transition is not without its challenges. In open surgery the physician can directly see and feel the anatomical structures. In image-guided procedures, the physician needs to identify anatomical structures in the images (segmentation), and mentally establish the spatial relationship between the imagery and the patient (registration). Additionally, the procedure's execution accuracy should be comparable or better than that achieved by the traditional approach (navigation). These requirements create a steep learning

curve, and increase the dependency of a favorable outcome on the physician's ability to mentally recreate the spatial situation and transfer a plan into action.

Image-guided systems aim at augmenting and complementing the physician's ability to understand the spatial structure of the anatomy by integrating medical images and other sources of information, such as tracked instruments. These systems potentially have a three-fold effect: (1) They can mitigate the learning curve for minimally invasive procedures and reduce the variability of the outcome, narrowing the gap between exceptional and standard practice; (2) They may enable new minimally invasive procedures, allowing physicians to perform procedures that were previously considered too dangerous; and (3) They transform qualitative procedure evaluations into quantitative ones, enabling a quantitative comparison between plan and execution.

Medical procedures are inherently an integrative process. Physicians mentally integrate their knowledge of anatomical structures with patient specific medical images to produce a plan and execute it. Image-guided systems use a similar approach, where all information sources are integrated and used to provide guidance to the physician.

Image-guidance systems were initially accepted by two medical disciplines, neurosurgery [77, 84, 124, 231] and orthopedics [53, 184]. The main reason for this early adoption is that both disciplines accommodate the use of a rigid anatomy assumption. In neurosurgery the brain's motion is constrained by the skull, although brain shift is an issue and has been the subject of much research. In orthopedics the assumption is always valid. Current commercial image-guided systems are all based on a rigid anatomy assumption. Image-guided systems for deformable anatomical structures are still a subject of research.

Previously published surveys on image-guided procedures include [74, 194, 246]. The intent of this review is two-fold: (1) to provide an updated view of the field of IGP and (2) to serve as a starting point for researchers interested in the technological components of IGP systems. We present an overview of the key technologies of IGP systems including references to relevant surveys in each technology area. We also describe the use of these technologies in research and commercial systems. Our review is limited to IGP systems that provide guidance using images and excludes image-less systems such as the Aesculap OrthoPilot [108]. We also do not discuss robotics related technology and systems which are described elsewhere [40, 247].

2 Overview of image-guided procedures

We describe image-guided procedures using a time-line based view. The three phases of a procedure are: pre-operative planning, intra-operative plan execution, and post-operative assessment. This is an idealized view, but it is useful in that it encompasses all the steps of an image-guided procedure. Each phase will now be described.

- **pre-operative planning**: In this phase the goal is to create a surgical plan based on pre-operative images and additional information such as implant geometry or

functional information. Multiple imaging modalities may be used concurrently, such as CT and MRI for optimal bone and soft tissue visualization, or CT and PET to correlate functional and anatomical data. Plans are formulated in a single coordinate system to which all data is mapped. These plans are patient and procedure specific and have variable complexity [208]. The complexity can range from simple plans such as specifying a target and trajectory for a biopsy [7], to moderately complex plans such as choosing and positioning implants [259, 111], to complex plans incorporating physically based simulations of joint movements [34] and interactions between soft tissue and bone structures [31, 272].

The key technologies involved in pre-operative planning are: (1) medical imaging and image processing, including correction of geometric and intensity distortions in the images; (2) data visualization, including the display and manipulation of image and data (e.g. implants); (3) segmentation, the classification of image data into anatomically meaningful structures; and (4) registration, the alignment of data into a single coordinate system so that corresponding points in all data sets overlap.

- **intra-operative plan execution**: Once the patient is in the operating room (OR), the coordinate system in which the plan was specified must be aligned to a coordinate system in the OR. The image-guided system now provides visual assistance to the physician, by tracking tools and anatomical structures and displaying their spatial relationships, using a variety of interfaces and displays. Additional information, such as intra-operative images, may be acquired to update the anatomical picture. If necessary, the procedure plan is then modified. During the procedure the guidance system can record the spatial relationships between the tools and the anatomy. This data can later be used for quantitative assessment of the intervention and for training purposes.

  The key technologies involved in intra-operative plan execution and update include all the technologies involved in pre-operative planning, in addition to: (1) tracking systems for localizing the spatial position and orientation of anatomy and tools; and (2) Human Computer Interaction (HCI), incorporating methods and devices for interacting with the guidance system and ways of conveying the information to the physician.

- **post-operative assessment**: Post-operative images are acquired and the results of the procedure are quantitatively compared to the pre-operative plan.

  The key technologies involved in post-operative assessment are the same as those involved in the pre-operative planning step.

3 Key technologies

From the discussion above we have identified the following key technologies involved in image-guided procedures:

1. Medical imaging, and image processing[1].
2. Data visualization.
3. Segmentation.
4. Registration.
5. Tracking systems.
6. Human Computer Interaction (HCI).

In the following subsections we will review each of these technologies, and their current state of the art.

3.1 Medical imaging and image processing

The main source of information for image-guided procedures are the medical images themselves. The first medical procedure to use images was performed in 1896, and utilized X-ray images. It is not clear who performed the first procedure, as evident from [74, 194]. What is clear is that the medical community had adopted this new technology within several months of its introduction. Medical imaging has come a long way since those first X-ray projection images, developed on glass plates, to today's digital tomographic images. Perhaps most indicative of the importance of medical images was the establishment of radiology departments in many hospitals early in the 1900's, shortly after the introduction of X-ray imaging.

Table 1 lists the common medical imaging modalities in terms of their availability for intra-operative use, their accessability, and data dimensionality. From this table it can be seen that for most procedures, physicians are still highly dependent on their ability to mentally reconstruct a three-dimensional scene based on two-dimensional intra-operative images.

We will now briefly describe each of these modalities[2].

Tomographic Images

All tomographic (3D) images consist of a set of two-dimensional cross sectional images which can be stacked together, to create a three-dimensional volume[3]. As the data is typically acquired using a slice based scheme the imaged object must be stationary throughout the acquisition process, or if the motion is systematic (e.g. respiratory or cardiac motion) gating can be employed. Ignoring the motion will result in distorted volumetric data as shown in Figure 1.

[1]This is low level image processing and not *image analysis*, which encompasses registration,segmentation, and functional analysis of anatomical structures [56].

[2]For a comprehensive review of current and prospective future imaging technologies the interested reader is referred to [278].

[3]An exception is 3D US utilizing 2D sensor arrays, which directly acquires 3D data.

Modality	Intra-operative Availability	Accessability	Data Dimensionality
Computed Tomography (CT)	available (not widespread)	high	3D
Magnetic Resonance Imaging (MRI)	available (not widespread)	high	3D
X-ray	available	high	2D projection
functional Magnetic Resonance Imaging (fMRI)	not available	moderate	3D
Positron Emission Tomography (PET)	not available	moderate	3D
Single Photon Emission Computed Tomography (SPECT)	not available	moderate	3D
X-ray Fluoroscopy	available	high	2D projection
C-arm CT	available	low	3D
Ultrasound (US)	available	high	2D
optical imaging	available	high	2D projection

Table 1: Classification of imaging devices according to their availability for intra-operative use, their accessability to physicians around the world, the dimensionality of the data they acquire and the type of information conveyed by the images.

The tomographic modality best suited for imaging bony structures is computed tomography (CT). This modality is considered to be geometrically accurate [138], but exhibits intensity artifacts when metallic objects are present in the field of view. These artifacts are the result of reconstruction using corrupted projection data, which is caused by the X-rays being greatly attenuated by the metal. There are a number of approaches to metal artifact reduction, including use of higher energy X-ray beams [210], and interpolating the missing projection data [114, 150, 213].

Intra-operative CT is available, but it is not in widespread use. A real-time version of this modality is CT-fluoroscopy, although most machines only provide the physician with a single image slice view that can be updated several times a second. The need for inexpensive intra-operative fully 3D data has led to the recent introduction of C-arm CT imaging [81, 276]. This modality utilizes iso-centric motorized C-arms to acquire a small field of view tomographic data set. Though the quality of the tomographic data is still lower than standard CT it is expected to improve with advances in C-arm image intensifier technology.

The main drawback of CT, CT-fluoroscopy and C-arm CT is their use of ionizing radiation [49, 115, 202]. Previously, it was hypothesized that there may be a threshold below which exposure to ionizing radiation does not increase the risk for cancer. A recent report from the US national academies suggests that this hypothesis is not valid and that risk of cancer proceeds in a linear manner with no lower threshold [1].

The tomographic modality best suited for imaging soft tissue is magnetic resonance imaging (MRI). MR images exhibit both geometric and intensity distortions. Geometric distortions are mainly caused by inhomogeneity of the main magnetic field and non-linearity of the magnetic field gradients [138, 237]. New MRI scanners incorporate geometric distortion schemes, so the end result may be sufficiently accurate for specific applications [12]. A recent evaluation of geometric distortions in clinical MRI systems

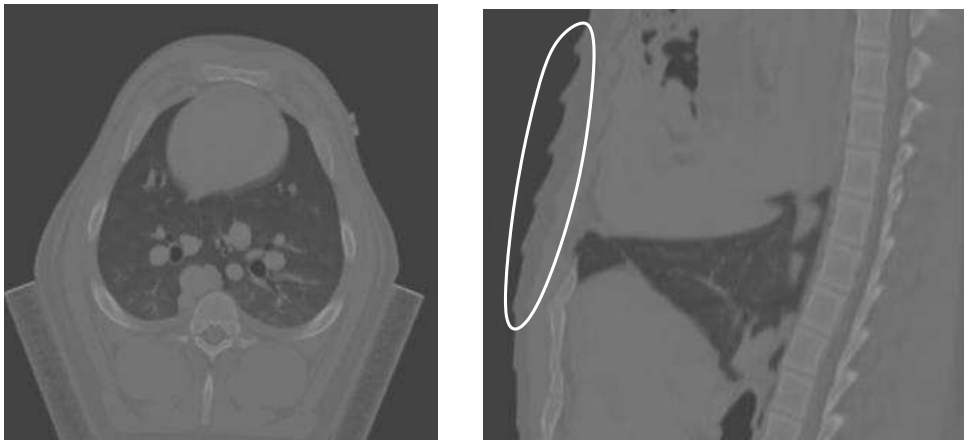

(a) (b)

Figure 1: CT data of breathing animal acquired with a single slice machine, (a) motion artifacts are not visible on a single slice (b) reformatted sagittal view of the volumetric data exhibits motion artifacts (skin surface should be smooth).

reports errors on the scale of several millimeters even when the machine's geometric distortion correction is applied [263]. For applications requiring better geometric accuracy, phantom based distortion correction schemes can be applied [54, 264], improving upon the machine dependent results. Intensity variations in homogenous tissue regions, can arise from gradient driven eddy currents, inhomogeneity of the main magnetic field and patient anatomy. Methods for correcting these distortions include among others, expectation maximization based bias field estimation [9, 269], parametric model estimation of tissue distribution and bias field [235], and more recently an iterative scale based approach [149].

Intra-operative MRI is available, although it is not in widespread use, mostly due to the requirement for specialized interventional suites. Additionally the quality of the images acquired by these systems is typically lower than that of standard MRI as they utilize low field magnets. These machines include the "double-doughnut" design [21], where the physician stands between the two magnets, and the open magnet design [233], where the physician has direct access to the patient from all sides, with limited access from above. Two recently introduced interventional MRI systems address the shortcomings of these older systems. The PoleStar (Medtronic Inc.) is a low field compact system that does not require a specialized suite of its own [88]. The systems' magnets are placed under the surgical table, and are raised into position only when images are required (Figure 2(a)). The Magnetom Espree (Siemens AG) is a high field "open bore" system. While its design is similar to conventional MRI systems, the machine's bore is much larger (70cm inner diameter) and the magnet is much shorter (120cm) enabling patient access(Figure 2(b)). For a comprehensive review of the current state of the art and future perspectives on interventional MRI the interested reader is referred to [110].

The tomographic modalities available for functional imaging are fMRI, PET, and SPECT.

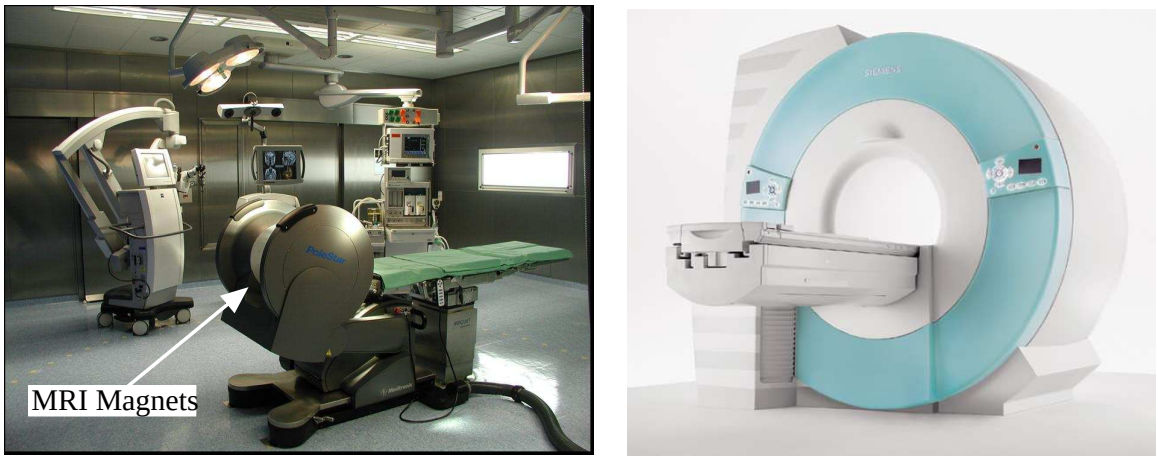

(a) (b)

Figure 2: Interventional MRI machines, (a) PoleStar system (courtesy D. Simon, Medtronic Inc.) and (b) the Magnetom Espree "open bore" system from Siemens AG (courtesy C. Lorenz, Siemens Corporate Research Inc.).

Although these are tomographic images the correlation between the functional data and the underlying anatomical structures is hard to discern. This is usually facilitated by aligning an anatomical data set to the functional one. Recently, combination PET/CT machines have been introduced, so that both modalities are available in the same coordinate system. Respiratory motion, however, is an issue since a PET image takes a long time to obtain ($> 1min$) so that resulting images represent an average over the breathing cycle [239].

Ultrasound is a highly flexible real-time modality for soft tissue and blood flow imaging. Ultrasound is not suitable for imaging the internal structure of bones or bodies of gas, such as the lung. The imaging hardware is very compact (Figure 3) and relatively inexpensive. Images are created by transmitting high frequency sound into the body and analyzing the echoes returned from the internal structures. Unlike other tomographic modalities data is acquired at arbitrary orientations, using free-hand scanning, and not as a stack of parallel slices. Ultrasound images are hard to interpret both due to their quality and the way they are acquired. Images usually exhibit variable contrast, image speckle, and shadowing artifacts. In addition, the data is acquired as a set of uncorrelated 2D images at arbitrary orientations, requiring the physician to mentally reconstruct the underlying anatomical structures, a task which is operator dependent.

Recently, 3D ultrasound has been gaining popularity as a means of mitigating the subjective interpretation associated with 2D free-hand scanning. Two approaches to creating 3D US data exist [63]: (1) using standard probes, 1D detector transducers, acquiring a set of 2D images coupled with their positional information, and (2) using 2D detector transducers, directly acquiring a 3D volume. The majority of systems use the former approach [76]. Acquiring a set of 2D ultrasound images with known positions is possible either by using mechanical positioning of the transducer, or free-hand, by incorporat-

Figure 3: The Terason compact ultrasound system from Teratech Corporation (MA. USA). Image shows all hardware components. System connects via IEEE-1394 (Firewire) to a laptop.

ing a tracking device mounted on the transducer. Finally, unlike all other tomographic imaging systems the US probe is in physical contact with the patient. This should be taken into account, as the scanning process may produce pressure-induced artifacts in the 2D images which in turn propagate into the 3D volume.

Projection images

X-ray fluoroscopy was introduced into medical use shortly after the discovery of X-rays. This modality is widely used in orthopedics and interventional radiology. Images are obtained using an image intensifier which is mounted on one side of a C shaped frame (C-arm) with the radiation source on the other side. This is a real-time modality with images being displayed on a screen, allowing the physicians to monitor the position of tools and anatomy. The images are characterized by a small field of view and exhibit geometric and intensity distortions [24, 58, 284], although newer machines exhibit these phenomenon to a lesser extent. Methods for correcting the geometric distortion either apply global correction schemes [58] or tessellations of the field of view followed by local corrections [284]. The main drawback of this modality is that it exposes the physicians to cumulative radiation [199, 228, 249].

Optical images are available from endoscopes and operating microscopes. Images may exhibit geometric and intensity distortions. The geometric distortion, in the case of endoscopes, is a radial (barrel) distortion, and is caused by the use of wide angle lenses. These type of lenses are used because they provide a large field of view, in an environment where camera motion is constrained (i.e. inside the body). Methods for correction of the geometric distortions are similar to those employed in X-ray fluoroscopy [4, 57, 95, 223]. Intensity distortions are due to specular reflections that are pose and lighting dependent. In many cases these distortions can be ignored, as changing the camera location will change the location of the specular highlights. Algorithms for detection and correction of specular highlights in a single image include color based methods [128], polarization

based methods [279], and hybrid color and polarization [179]. Use of multiple images from the same viewpoint under different lighting conditions is also possible [64], with the recently introduced concept of multi-flash imaging [201, 245].

3.2 Data visualization

Once images are acquired they can be viewed in conjunction with additional information (e.g. models of tools). Projection images are displayed as is, with additional information such as tool locations or underlying anatomical structures superimposed onto the image. Tomographic images are visualized in one of three ways: surface rendering, volume re-slicing, and direct volume rendering (DVR). Surface rendering and methods for DVR that incorporate segmentation are the only approaches that explicitly visualize individual anatomical structures. Volume re-slicing and most DVR methods defer the task of identifying anatomical structures to the user. As visualization is done in 2D, displaying images on a screen, more than one view is required to facilitate the understanding of the underlying 3D anatomical structures. Usually, two or three orthogonal views are sufficient.

The goal of data visualization in image guided procedures is to *concisely* convey the relevant information for the successful completion of the intervention. Traditionally, physicians are taught to mentally reconstruct anatomical structures based on axial, sagittal and coronal slices. As volume re-slicing creates these familiar views, physicians tend to prefer this type of visualization over surface rendering or DVR. We expect this preference to change with the growing use of three-dimensional visualization as part of the medical training curricula.

Next, we briefly describe each of the visualization techniques.

Surface rendering

Surface rendering is an indirect method of visualizing the anatomical structures from a tomographic data set. It is the most popular rendering method in computer graphics, with images usually generated at interactive rates on dedicated hardware. Surfaces are most commonly represented by polygonal meshes, although other representations are possible (e.g. NURBS). The rendered images are either perspective or orthographic projections of the surfaces [70]. A prerequisite of this approach is the segmentation of meaningful surfaces from the volumetric data, with rendering accuracy dependent on segmentation accuracy. The resulting mesh sizes are sometimes too large for interactive rendering. To overcome this problem, surface simplification algorithms are applied [145], and the resulting simplified mesh is used for display. This visualization method best facilitates the display of specific anatomical structures and interaction with them, as its inputs are anatomically meaningful structures obtained by segmentation.

Volume re-slicing

Volume re-slicing is the simplest visualization method. An image is created by positioning a uniform rectilinear planar grid that intersects the original volume. Intensity

values are estimated at the grid points using interpolation [163]. This yields a 2D slice through the volume which is not necessarily parallel to the original acquisition plane. Image quality depends on the combination of grid spacing and interpolation method. In most cases, the rendered images are the standard axial sagittal and coronal views of the anatomy. Arbitrary planes are seldom used, as physicians find it hard to infer the underlying anatomical structures from views that they are unfamiliar with. Visualizing the rendered images in conjunction with additional 3D information such as surface models is done by texture mapping the image onto a rectangular polygon [70] positioned at the location of the sampling grid. As current standard monitors are only capable of displaying 256 shades of gray and pixel values can exhibit a larger range, a value ,v, is usually mapped to the interval $[0, 255]$ via the window ,w, and level ,l, mapping:

$$f(v) = \begin{cases} 0 & l - 0.5w > v \\ \left[255\frac{v-l+0.5w}{w}\right] & l - 0.5w \leq v \leq l + 0.5w \\ 255 & l + 0.5w < v \end{cases}$$

Finally, it should be noted that this visualization method does not enable display of specific anatomical structures and interaction with them, as the volumetric data is treated as a single object.

Direct volume rendering

Direct volume rendering (DVR) methods are a set of techniques that generate images without requiring explicit segmentation of structures from the volumetric data. The rendered images are either perspective or orthographic projections. In most cases, interaction and rendering of individual anatomical structures (e.g. a specific vertebral body from a volume containing the spine) is not possible, with the exception of hybrid methods that explicitly incorporate segmentation.

Although no explicit segmentation is required, all the techniques require the definition of a transfer function, a mapping from volume data to color and opacity values. This function can be viewed as a fuzzy segmentation, although in general it does not segment the data into anatomically meaningful structures. The transfer function's input can be the volume intensity values, the volume gradients, an iso-value, or an explicit segmentation. Choosing a transfer function is the most important component of DVR, as it defines what is displayed. How to choose an appropriate transfer function for a given data set is still a research subject with options ranging from manual to fully automatic [195].

DVR methods are classified into two main categories [119] : image order and object order. Image order methods traverse the pixels and determine which voxels contribute to the pixel value. Object order methods traverse the voxel data and map it to the image. Hybrid approaches also exist, with the most popular one being the shear-warp algorithm [131].

Image order methods, also known as ray casting, generate images by sending a ray through each pixel into the scene and sampling the volume data along the ray. Color and opacity values at the sample points are computed via interpolation from neighboring grid points, and merged to give the pixel color. The resulting image depends on the

combination of sampling method, interpolation method, and merging method. Sampling methods include uniform sampling [141], adaptive sampling [46], and discrete voxel traversing [282]. Interpolation methods have been studied extensively [136, 153, 163], with methods ranging from nearest neighbor and linear interpolation through B-spline to methods that ensure error bounds [148]. Merging methods include selection of maximum value, summing all values, or alpha composting among others. Specific combination choices for sampling, interpolation, and merging arise from different requirements on spatial accuracy, rendering speed, and ability to highlight specific anatomical structures.

Object order methods traverse the voxel data and map it to the image. The two most popular methods from this category are splatting and hardware based texture mapping [164, 221]. Splatting [273] generates images by using a kernel function reconstruction of the volume that is projected onto the image plane. The original volumetric signal is reconstructed using overlapping kernel functions, usually finite extent Gaussian kernels, centered on the grid points with amplitude scaling according to the intensity value. Each kernel function is projected onto the image plane by integrating it along the viewing direction to give a 2D footprint. Efficient projection of the kernel functions can be achieved using a pre-computed footprint, with the quality of the image depending on the type of reconstruction kernel, its extent, and the resolution of the footprint table. Hardware based texture mapping [27] is performed by loading the volume into texture memory, rasterizing polygonal slices parallel to the viewing direction and merging them. The rasterization process is equivalent to the software based volume re-slicing approach described above. The choices of merging methods are equivalent to those used for ray tracing.

Traditionally, the two main drawbacks to DVR have been slow rendering speeds and the inability to interact with distinct anatomical structures. These drawbacks are overcome by methods that combine the results of segmentation with the rendering process [25, 83]. Segmentation is used as a filter, defining sub-volumes of interest. Dilation and erosion operators can be applied, expanding or contracting the volume of interest, either to include surrounding structures of interest or to overcome segmentation errors. Interaction with the individual anatomical structures is possible via the underlying segmentation.

3.3 Segmentation

In the context of IGP, we define segmentation as a partitioning of the image domain into non-overlapping connected regions that correspond to distinct anatomical structures. While segmentation of medical images has been studied extensively [6, 196], no automatic technique has been found to be applicable across imaging modalities and anatomical structures [56]. Therefore, the task of segmentation can be considered complete only when the physician judges the results to be satisfactory.

Given this practice we divide segmentation algorithms into two categories: (1) algorithms where the user can explicitly specify the desired segmentation; and (2) algorithms where the specification is implicit.

The first category views segmentation as an interactive process where the user is provided with real-time feedback and directly modifies the segmentation until satisfactory results are obtained. Very few interactive segmentation algorithms have been developed, as many researchers equate interaction with labor intensiveness. In practice all segmentation algorithms involve some form of interaction [185], even autonomous algorithms usually require parameter setting or manual post processing to obtain correct results. We identify two types of algorithms in this category, manual segmentation and user steered segmentation.

Purely manual editing is too labor intensive for use in a clinical setting, and with the continued growth in size and resolution of data sets it will soon become impractical even for research purposes. Although impractical on a large scale it is still a valid post processing approach, where it is used to modify results obtained by more autonomous segmentation methods. Two recent examples of this approach are [117] and [107]. In [117] the user edits the segmentation results by selecting a volume of interest and then either applying mathematical morphology operators, local thresholding, or directly manipulating the surface to achieve the desired segmentation. In [107] a rational Gaussian surface is fit to the segmented object and the user directly manipulates the surface representation to correct segmentation errors.

Algorithm steering is based on real-time interaction between the user and algorithm, where the user views the segmentation results and explicitly steers the algorithm to a desired segmentation. In the extreme this framework degenerates to manual segmentation, with the user forcing a specific result. Examples of this approach are the livewire family of algorithms for 2D [60, 173] and 3D [59, 219] segmentation. These algorithms produce a piecewise optimal boundary representation of the object, by viewing the image as a weighted graph and finding the shortest path between consecutive user specified boundary points. A more recent example of this approach based on the concept of random walks is described in [80]. Again, the image or volume are viewed as a weighted graph. The user marks a small number of pixels per object and background. An unclassified pixel is then labelled according to the probability that a random walk starting at its location first reaches one of the user labelled pixels.

The vast majority of segmentation algorithms fall into the second category, methods where the user cannot explicitly specify a desired result. These include, among others, thresholding, edge based methods, region based methods, markov random fields, level set methods, atlas based methods, and deformable models with or without learning. Several general surveys on medical image segmentation have been published [6, 196], with specialized surveys on deformable models [161, 169, 242], vessel extraction [126, 240, 241], and brain segmentation [243, 244] also available.

Automated segmentation of medical images is a hard task. Images are often noisy and usually contain more than a single anatomical structure with small distances between organ boundaries. In addition the organ boundaries may be diffuse. To deal with these challenges, many algorithms incorporate domain specific prior knowledge. In its most limited form this leads to an educated weighting of the different terms of a generic

optimization functional such as in the original active contours approach [118]. Another approach is to tailor the optimization functional to specific types of structures. Recent examples of this approach include segmentation of small blood vessels [283], and sheet like osseous structures [52].

A more constrained framework to segmentation, which incorporates anatomic specific knowledge, replaces the task of segmentation with registration of pre-segmented models. These models are either patient specific, atlas based, or statistical models of appearance. A nice intrinsic characteristic of this approach is that results are guaranteed to be topologically correct, assuming the model is not allowed to change its topology during optimization.

In its most basic approach the model is patient specific. That is, given an instance of the anatomical structure in one modality the goal is to segment it in another modality. Once the model is registered it defines the segmentation. In this approach registration simply transfers a known segmentation to another data set. An example of this approach is [92], where a CT based vertebral model is registered to an X-ray image. The tasks of segmentation and registration are coupled via an iterative scheme. Segmentation results are ranked according to the current registration estimate and an incremental registration update is computed based on the segmentation.

Extending this approach, the patient specific model is replaced with an atlas. The atlas is registered to a new patient specific data set, producing a segmentation. As the model is generic, registering it to patient specific data requires the use of curved (deformable) transformations. While the combination of an atlas and curved transformations enables segmentation of structures that differ significantly from their atlas based representation, it can also lead to erroneous results if the transformation parameters are unconstrained. This approach has mainly been applied to segmentation of brain structures using different variants of deformable registration [37, 48, 258].

Statistical models of appearance are anatomy and modality specific models that encode variations in shape and intensities as captured by a set of segmented training images. The most popular model representation is based on point distributions. These are commonly known as active shape models (ASM) [42] and active appearance models (AAM) [43], with ASM encoding the objects boundary, and AAM encoding the boundary and intensities inside the object. ASM based segmentation has been applied to a variety of anatomical structures and modalities including: vertebra in X-ray images using 3D models [14], prostate in MR using 2D models [44], heart in MR using 3D models [143], and femur in X-ray images using 2D models [13]. Similarly, AAM based segmentation examples include: heart in MR using 2D models [232], heart and lungs in X-ray images using 2D models [257], and heart in US and MR using 3D models [168].

Models are constructed using a set of training images with corresponding landmark points marked on each of the images. Shape and intensity parameter spaces are described by the modes of variation obtained by principle component analysis of the training data. The main challenge with this approach is the need for automatic specification of landmarks on all training images. A method that provides an optimal solution to

this challenge is described in [47], where the optimal model is defined as the one that minimizes the description length of the training set.

The task of segmentation is then cast as an optimization of an appropriate similarity measure where the optimized parameters include object pose, shape, and possibly intensity. When only pose and shape are optimized the approach is equivalent to registration with constrained deformation. In general, both shape and intensity variations are constrained to the sub-space defined by the modes of variation computed from the training set. This is both beneficial and detrimental. It is beneficial, as the training set enforces reasonable constraints on possible object appearance. It is detrimental when the constraints are too limiting. This occurs when the training set does not span the space of all possible variations. One solution to this problem is to incorporate the statistical model based approach into a general deformable model, striking a balance between the constraints imposed by the training set and generic physics based deformations [120].

3.4 Registration

Registration is defined as the alignment of multiple data sets into a single coordinate system such that the spatial locations of corresponding points coincide. Registration has been studied extensively both for medical and non medical applications [79, 91, 97, 134, 151, 288] and is still a very active area of research. To evaluate the suitability of a registration for image-guided procedures we consider three factors: (1) accuracy, as measured by the target registration error (TRE) [69], which indicates how far the predicted position of the anatomical target is from its actual position (2) speed, or how long does it take the algorithm to produce the solution and (3) robustness, or how well does the algorithm deal with noise and outliers. The requirements for accuracy and robustness are equivalent in all stages of the procedure, with TRE's on the order of several millimeters deemed sufficient for most medical procedures. Requirements on the speed of an algorithm are stringent in the intra-operative stage, with a solution required within several seconds to a couple of minutes. This time constraint can usually be relaxed for the other procedure stages.

Registration methods can be categorized according to many criteria [151], which fall into two general classes: input related, and algorithm related. Input related criteria are:

- Information involved: combinations of image modalities, models and data obtained by tracking devices.
- Data dimensionality: combinations of 2D and 3D (e.g. 3D/3D CT to MR, 2D/3D X-ray to CT).
- Data source: either from the same patient, different patients, or an atlas.
- Anatomy: which anatomical structures are registered, osseous or soft tissue (e.g. femur, liver).

Algorithm related criteria are:

- Transformation type and domain: the transformation type can be rigid, affine, projective, or curved, and the domain can be local or global.
- Feature types: combinations of feature types (e.g. points to surface registration). Features are either extrinsic (typically using specially designed fiducials) or intrinsic (anatomy based). They can be geometric entities (i.e. points, curves, surfaces), image intensities, or image gradients.
- Optimization method: analytic or iterative.
- User interaction: the amount of user interaction required for registration, usually divided into three categories: interactive (manual optimization of similarity measure), semi-automatic (user initialization of optimization), and automatic.

As most image guidance systems only incorporate rigid registration we limit our review to this category of algorithms. Deformable registration methods for image-guided procedures are still a subject of research and will only be described briefly, in the context of brain shift compensation[4].

The most popular and mature registration methods used in image-guided surgery are those that fall into the categories of 3D/3D, point/geometric entity, rigid registration. These methods are based on paired point registration where the pairing is either known or computed.

Analytic, least squares, algorithms using known point pairs for rigid registration have been in use for over two decades, with the most popular ones representing rotations either as matrices [3, 103, 224, 254] or unit quaternions [61, 102]. Error analysis and prediction for these methods is well understood [69, 68], making them especially suitable for medical procedures, where knowledge of expected errors is of utmost importance.

Most image-guided systems incorporate fiducial based registration using these algorithms. Pre-operatively and post-operatively registration is used to align complementing image data sets (e.g. CT/MR). Intra-operatively registration is used to align the pre-operative image coordinate system with the intra-operative coordinate system. Two types of fiducials are available: implantable and skin adhesive (Figure 4). Implantable fiducials require an additional surgical procedure and facilitate accurate registration that can also be used as a gold standard for validation of other registration methods [270]. Skin adhesive fiducials do not require additional surgery, but yield less reliable registration results as they may move due to skin motion between data acquisitions. A fiducial-less approach is also possible, by identifying corresponding anatomical landmarks in the two modalities. This approach is the least accurate, because the number of landmarks appearing in both modalities is usually small, and their localization is error prone.

Algorithms that do not require prior knowledge about the point correspondences were independently introduced in [287], [35], and [15], with the later work coining the name

[4]For a review of deformable registration algorithms the interested reader is referred to [139].

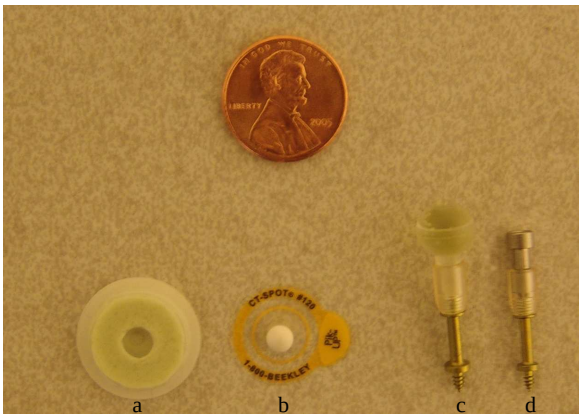

Figure 4: Registration fiducials: (a) CT/MR compatible adhesive skin marker from IZI Medical Products Corp., Baltimore MD, USA; (b) CT compatible adhesive skin marker from Beekley Corp., Bristol CT, USA; (c,d) Acustar II CT/MR compatible implantable markers with interchangeable caps from Z-kat, Hollywood Fla, USA, manufactured by Stryker, Kalamazoo MI, USA (c) with imaging cap and (d) with conical cap for pointer based digitization (implantable markers courtesy of J. M. Fitzpatrick).

iterative closest point (ICP). These works describe an iterative procedure where point correspondences are established and an analytic least squares method is used to compute incremental transformations whose composition is the desired transformation. In [15] and [287] point correspondences are established based on the minimal Euclidean distance (closest point) although, as noted in [215], the framework they introduced can use other pairing approaches. Table 2 summarizes the general framework.

In practice, the original framework suffers from several deficiencies: (1) point pairing is a speed-wise expensive operation; (2) convergence is local, requiring an initial transformation near the correct one; and (3) the framework is highly sensitive to outliers and non-Gaussian noise because the incremental transformations are computed using a least squares approach. A large body of papers addressing these issues exists. Methods for accelerating the running time include, use of a kd-tree spatial data structure [15, 82, 225], closest point caching [225], extrapolation of the transformation parameters [15, 225], approximate nearest neighbor searches [82], parallelized nearest neighbor searches [132], hierarchical coarse to fine approaches [287, 112], and combinations of these methods. Methods of initialization include manual alignment and use of known paired points with relaxed requirements with regard to localization accuracy. Robust versions of the ICP algorithm include, use of simulated annealing [78, 144, 192], M-estimators [116, 147], least median of squares [156, 252], least trimmed squares [36], and weighted least squares [157, 253, 287].

Applying these algorithms using points acquired from anatomical structures is a common approach in image-guided surgery. For pre-operative and post-operative 3D/3D registration the points are usually obtained as a result of segmentation. For intra-operative registration the points are usually acquired by touching the anatomical structures us-

0. Initialization:
   (a) Set cumulative transformation, and apply to points.
   (b) Pair *corresponding* points and compute similarity (e.g. root mean square distance).
1. Iterate:
   (a) Compute incremental transformation using the current correspondences (e.g. analytic least squares solution).
   (b) Update cumulative transformation, and apply to points.
   (c) Pair *corresponding* points and compute similarity.
   (d) If improvement in similarity is less than threshold τ or number of iterations has reached threshold n terminate.

Table 2: Iterative Corresponding Point (ICP) framework

ing a tracked probe. This method has two main drawbacks: it is invasive and point acquisition is limited to the exposed parts of the anatomy. A less popular, non invasive method, for point acquisition is based on segmentation of intra-operative US images [96]. The reasons for its limited popularity are that it requires additional hardware, an US machine, and accurate localization of points corresponding to the anatomical structures in the US images is a hard task.

An alternative non-invasive approach to intra-operative point based rigid registration is the use of projection images and 2D/3D registration. This approach replaces the intra-operative acquisition of surface points with the acquisition of one or more X-ray projection images. Several categories of 2D/3D algorithms exist: geometric feature-based [16, 87, 92, 127, 135], intensity-based [98, 122, 129, 133, 137, 177, 193, 216, 289], and hybrid approaches [142, 250]. All these algorithms are iterative and require initialization. The initial transformation can be obtained in several ways: 1) from the clinical setup, according to the patient's position on the operating table (e.g. supine), and the intra-operative imaging views (e.g. AP); 2) using skin adhesive fiducials and paired point registration; and 3) using anatomical landmarks that are identified on several images, estimating their location via triangulation and performing point based registration.

The geometric feature-based approach consists of four steps: 1) feature extraction, choosing the features of interest in each data set; 2) feature pairing, establishing correspondences between the features of each data set; 3) dissimilarity formulation and outliers removal, quantifying the dissimilarity between paired features, using metrics such as sum of pairwise distances; and 4) dissimilarity reduction, finding the transformation that optimally minimizes the dissimilarity. Steps 2)-4) are repeated until convergence.

The intensity-based approach consists of three steps : 1) image formation, creating a simulated projection image based on the 3D data, also known as a Digitally Reconstructed Radiograph (DRR) ; 2) dissimilarity formulation, quantifying the dissimilarity between the simulated and actual projection image using a metric such as normalized mutual information; and 3) dissimilarity reduction, finding the transformation that optimally minimizes the dissimilarity. Steps 1)–3) are repeated until convergence.

Geometric feature-based algorithms are usually faster than intensity-based algorithms, but their accuracy and robustness are usually worse [162]. These differences can be attributed to the amount of original data used by each approach. Feature-based methods use less of the original data. This leads to lower computational complexity, but at the same time their accuracy and robustness are limited by the accuracy and reliability of the feature extraction and established correspondences. Intensity-based methods on the other hand use all the data. This leads to higher computational complexity, mainly due to the process of DRR generation, but this makes intensity-based methods potentially more accurate and robust.

Many researchers have addressed the disadvantages of each approach while attempting to maintain the advantages. In the feature-based approach emphasis has been placed on obtaining better segmentation and correspondence results. This can be achieved by combining the registration and segmentation into an iterative framework. The current estimated registration is used to drive the segmentation and correspondence creation, which in turn are used to compute the new registration estimate [8, 92]. In the intensity-based approach emphasis has been placed on speeding up the DRR generation process. The popular approaches for speed improvement are: (1) partial image generation, either regions of interest [129, 177], or random sampling [289]; (2) light field rendering, precomputation of the line integrals of a large set of rays and approximation of the DRR generation using the light field data structure[5] [133, 129, 216]; (3) accelerated rendering using the graphics processor [133, 122, 217]; and (4) multi-resolution approaches [129, 193]. Combinations of these acceleration methods have also been used.

Finally, there exist hybrid registration approaches which are not directly based on intensity or geometric features [142, 250]. These approaches use a small set of rays for computation, but avoid explicit segmentation by using the relationship between the 3D and 2D image gradients. They are therefore faster than intensity-based methods, and are potentially as accurate and robust. A recent comparison study [256] between the hybrid algorithm presented in [250] and the intensity method presented in [193] concluded that their accuracy is comparable, with the hybrid method being an order of magnitude faster.

Image-guided systems incorporating non-rigid registration have mostly been developed for neurosurgical procedures. These systems provide feedback using high quality preoperatively acquired MRI scans. During open cranial surgery the brain may shift (deform) by more than $10mm$ [93, 209]. Once brain shift occurs accurate navigation using

[5]This data structure appears in the literature under several different names: light field, lumigraph, transgraph, or attenuation field.

the pre-operative volumetric data is only possible if it is updated so that it is consistent with the intra-operative situation. Non-rigid registration between the pre-operative volume and intra-operatively acquired data enables this update.

Two sources of intra-operative data for monitoring brain shift exist: brain surface reconstructions and tomographic data. Surfaces are estimated by either using laser range scanning [5, 167, 226], or stereo based reconstruction methods [189, 229, 238]. Tomographic data is acquired using tracked US [41, 140, 146], or interventional MRI [39, 266]. While interventional MRI can potentially provide sufficient guidance on its own, use of pre-operative MRI is preferred as it provides higher quality images (higher resolution and SNR).

Systems that perform surface reconstruction are inexpensive and utilize widely available hardware. They operate under the premise that knowledge of surface deformation is sufficient for correct deformation estimation throughout the volume, a feasible assumption if the surface data is used in conjunction with bio-mechanical models of deformation, such as in [89, 190].

Systems that use tomographic data for intra-operative monitoring are inexpensive and widely available, in the case of ultrasound, and expensive and not in wide spread use, in the case of interventional MRI. While ultrasound is low cost and widely available it suffers from two deficiencies:(1) image quality is relatively poor; and (2) imaging requires tissue contact. This later requirement limits its use to cases where the craniotomy is large enough for the placement of the US probe and the scanning process may induce additional pressure related deformations. Non-rigid registration methods based on tomographic data employ either bio-mechanical models [146, 265] or generic physically motivated non-rigid registration algorithms [41].

3.5 Tracking systems

Tracking systems are used to determine the position and orientation of tools and anatomical structures in image-guided procedures. Tracking technologies used in medical applications include encoded mechanical arms, optical ego-motion (self-motion) tracking, fiber optic based devices (ShapeTape^{TM}), optical tracking, electromagnetic tracking, and ultrasonic based tracking. Reviews of some of these technologies and their characteristics can be found in [74, 194, 204]. For a comprehensive review of tracking technologies, not specific to medical applications, we refer the reader to [268].

Tracking devices can be divided into two classes, devices that can only track a single object at a time, and those that can track multiple objects concurrently. The former include encoded mechanical arms, optical ego-motion tracking, and the ShapeTape^{TM} device. This ability separates the systems into those that are flexible enough to be used in a variety of procedure types and those that are limited to certain procedures, usually requiring patient immobilization. This flexibility is the main reason for the current dominance of optical and electromagnetic tracking systems in medical applications.

To understand the factors contributing to the widespread acceptance of optical and

electromagnetic tracking we will first define the ideal tracking system for IGP and then describe the different technologies as they relate to this ideal system. Following [268], the ideal tracking system is defined as:

- Small: an unobtrusive system.
- Complete: estimates all six degrees of freedom.
- Accurate: resolution less than $1mm$ and 0.1^o.
- Fast: refresh rate of 1,000Hz with a latency of less than 1ms, regardless of the number of deployed sensors.
- Concurrent: tracks up to 100 objects concurrently.
- Line of sight: does not require line of sight.
- Robust: not affected by the environment (light, sound, magnetic fields, etc.).
- Working volume: has an effective work volume of 5^3m (room sized).
- Wireless: sensors are wireless and can function for several hours.
- Inexpensive.

Encoded mechanical arms have been used mostly in neurosurgical procedures, where the patients head is traditionally restrained [203, 227]. These devices are large and rather cumbersome. The pose of the object of interest is estimated with sufficient accuracy and refresh rates for medical procedures. The main drawbacks of using a mechanical arm are that only a single object can be tracked at a time and that these systems can be awkward and time consuming to use. These drawbacks can be traced to their original intended use as portable coordinate measuring machines. The devices do not require line of sight, they are robust to environmental changes, and have sufficient work volumes for most medical procedures. This system type is inherently wired, as the tool pose at the end of the device is computed from the knowledge of joint parameters and link lengths. A recent comparison between an optical tracking system (FlashPoint 5000) and mechanical tracking system (FAROArm) [154], found that their performance is comparable, but that the optical system is more appropriate for intra-operative use due to ergonomic issues and the need for patient fixation when using the mechanical arm.

Optical ego-motion (self-motion) tracking utilizes video to compute camera motion [26, 51, 170]. This technology has been used in endoscopy-based navigation systems, although any tool that is rigidly attached to a camera can use the technique, once the camera to tool transformation is computed (i.e. hand eye calibration). As this approach requires that a camera be attached to every tool it is best suited for endoscopic procedures where a camera is already in use. The tracking is thus unobtrusive as it uses already available data. The systems are able to estimate all six degrees of freedom with

accuracy dependent on the image content. In the case of uniform image content tracking is not possible, although this is rarely the case. An important assumption of all tracking systems is that all object motions are rigid, which is not always true since anatomical structures can deform, particularly soft tissue organs. As ego-motion systems depend on this assumption images where the anatomy is deforming will result in inaccurate tracking.

The ShapeTape^{TM} is a unique device that uses fiber optic technology to estimate the location and orientation along its length [186]. The tape is attached to a structure and tracks the shape of the structure as it moves. It is relatively unobtrusive, with accuracy dependent upon the tape length. Object poses are computed at real-time rates, but it can only report on a single object at a time. The work volume depends on the tape length and is related inversely to accuracy. The tape can either be connected directly to the data acquisition system or via a wireless connection.

Optical tracking systems use camera rigs to track fiducial markers that are attached to the instrument or anatomical structure of interest [248, 285]. Camera rig sizes vary, with the extremes being the large Optotrak (1126x200x161mm) and the small MicronTracker2 (172x57x57mm) systems (Figure 5(a) and (b)). Fiducials include infrared light emitting diodes (IREDs) (e.g. FlashPoint 5000), reflective fiducials that are illuminated with infrared light (e.g. Polaris), and markers that exhibit high contrast in the visible spectrum (e.g. MicronTracker2). To estimate object pose at least three fiducials are required. Fiducial localization accuracy is sub-millimetric for all optical systems, although the accuracy at the tip of an instrument varies according to the fiducial configuration [271]. All systems provide real-time refresh rates that are sufficient for medical procedures, and can concurrently track multiple objects. Their main drawback is the line of sight requirement. This limits their use to rigid instruments, and can also be cumbersome as the line of sight can be inadvertently occluded by hospital personnel during the procedure. Their performance is robust with regard to the environment, and they provide sufficient working volumes for most medical procedures. Systems are either wired, using IREDs, or wireless, using IREDs, reflective fiducials or marker patterns. Wireless systems are usually preferred as they are less cumbersome. However wireless systems require that a unique fiducial configuration be associated with every tool, which is not necessary when using a wired system.

Electromagnetic tracking systems consist of a transmitter (field generator) and sensor coils that can be embedded into the tracked objects [11, 18] (Figure 5(c)). Transmitter sizes are small (e.g. microBird 96x96x96mm), and receiver sensors have diameters in the range of $1mm$, making it possible to embed them into small tools. Two types of sensors are available, 6D sensors, that estimate all pose parameters and 5D sensors that estimate all parameters except rotation around the long axis of the coil. Sensor localization and orientation accuracies are in the $1mm$ and 0.5^o ranges. Refresh rates are sufficient for most medical procedures with multiple objects tracked concurrently. The main attraction of electromagnetic tracking is that no line of sight is required. This enables the system to track instruments inside the body, without the rigid instrument constraint associated with optical tracking. Dependent on the required accuracy

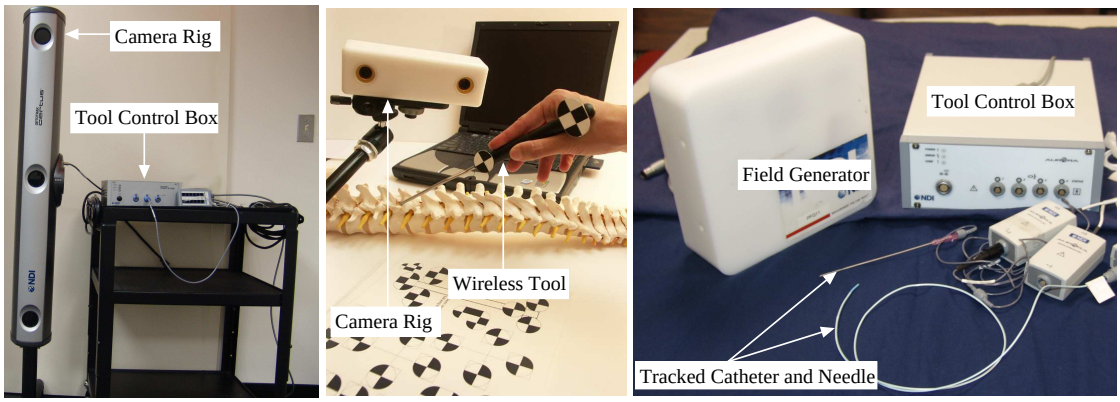

Figure 5: Tracking systems, optical: (a) Optotrak Certus (Northern Digital Inc., Waterloo ON, Canada), (b) MicronTracker2 (courtesy Claron Technology Inc., Toronto ON, Canada); and electromagnetic: (c) Aurora (Northern Digital Inc., Waterloo ON, Canada)

flexible instruments can be tracked by either embedding multiple sensors into them, or only tracking the tip as it advances inside the body. The main drawback of these systems is that their accuracy degrades in the presence of metallic objects that distort the magnetic field. This issue has drawn much attention, both from manufacturers and users. Manufacturers have strived to make their systems "metal immune" with some recent success, as evident when comparing older accuracy evaluations [17, 105] to more recent ones [106, 220]. Users have also addressed this issue by developing a variety of in-situ correction schemes [125, 178, 280, 38] using mechanical devices, robots, and optical tracking systems to establish ground truth. It should be noted that all in-situ correction schemes assume that the environment does not change between calibration time and procedure time, an invalid assumption if distortion inducing surgical tools are being used. An additional drawback of electromagnetic tracking systems is that they are wired, although this has recently changed with the introduction of the wireless system from Calypso Medical Technologies Inc. (Seattle WA, USA) [188, 286].

Ultrasonic systems work by attaching emitters, sound point sources, to the objects, and using the time of flight between source and a number of detectors to estimate the location of the source [72, 205]. The systems are unobtrusive, and compute object pose with sufficient accuracy for medical applications. Unfortunately, this approach requires that a single emitter fires at a time, and that there be a time delay between them in order for their location to be estimated. This is why reliable pose estimation is mostly limited to static objects. Multiple objects can be tracked concurrently, but the single emitter at a time constraint sets hard limits on the object motions. In addition to these constraints these systems also impose the line of sight constraint between emitters and detectors. Work volumes are sufficient for medical procedures, and the systems are wireless. However, ultrasonic systems are rarely used in image-guided systems.

3.6 Human Computer Interaction (HCI)

We divide the technologies associated with HCI into two categories: interaction techniques and information presentation. Early IGP systems did not place much emphasis on HCI. User input was based on using the standard keyboard and mouse and information was presented on standard computer monitors using the traditional anatomical representations of axial, sagittal, and coronal volume slices. While this approach may be acceptable for the pre and post operative stages it is problematic for intra-operative use. Intra-operatively it is difficult for the physician to interact directly with the system [262]. The keyboard and mouse cannot be sterilized, and even if it were possible to sterilize them they are too cumbersome for use in the the crowded environment near the patient. In addition, the use of a standard monitor to display information results in perceptual discontinuity as the physician's focus must alternate between patient and display. Finally, we note that the use of standard anatomical views is not optimal for all interventions.

For IGP systems to gain wider use the physician must be able to directly interact with the system without having to use a keyboard or mouse. Several approaches to achieve this goal exist including touch screens, trigger like input devices such as foot switches, tracked virtual keypads, speech recognition systems, and computer vision based gesture recognition techniques. Speech and gesture recognition techniques are currently in limited use due to safety issues, as their input is based on recognition algorithms which currently do not guarantee 100% recognition rate under the conditions found in the operating room.

Touch screens replace the keyboard and mouse by integrating their functionality into the display. The screen is covered with a sterile drape allowing the physician to touch it during the procedure. While this approach provides a means for complex interaction, it requires that the screen be placed near the physician, which can be difficult in the crowded procedure room.

Binary input devices such as foot switches and tool embedded switches function as event triggers. Although they do not enable complex interactions, they provide sufficient control in many situations. A common situation that requires this type of interaction is the acquisition of data from external devices at a specific point in time, for instance, point acquisition for intra-operative registration. In this situation, the physician uses a tracked probe to acquire point locations. As the probe is continuously tracked, triggering an event notifies the system that it should acquire the current point. Similarly, the system can be notified that an intra-operative image has been acquired by an imaging device and that it should be uploaded.

The tracked virtual keypad [262] addresses the two issues precluding the intra-operative use of keyboard and mouse as it is sterilizable and relatively unobtrusive. The keypad itself (Figure 6) can be customized on a per-procedure basis so that the virtual keys represent only the commands that are relevant for that procedure. This approach encodes all the relevant interaction into a minimal form factor. Additionally, as key-press events are generated based on the proximity of a tracked tool to the virtual key location, any

Figure 6: Virtual, tracked, keypad (courtesy N. Glossop, Traxtal technologies).

tracked tool can be used to activate the commands.

Speech recognition systems provide the same functionality as the virtual keypad [262]. They are either user dependent [262, 218], requiring training per user, or user independent. Although user dependence is usually viewed as a deficiency, in IGP it can be viewed as an additional safety measure, ensuring that actions are performed only if a specific physician gives the command [262]. Additionally, to ensure that commands are only invoked intentionally, use of a keyword to prime the system before issuing commands is possible [130].

Computer vision based gesture recognition techniques aim at providing direct and intuitive interaction between users and machines [2, 191, 197, 281]. Gestures are either communicative or manipulative [197] and can be classified as dynamic, motion based, or static, pose based. Although these systems show great promise, they are still not robust enough for use in most IGP systems. To achieve widespread use these techniques must achieve a recognition rate of 100% using images exhibiting lighting changes and clutter, both of which are inherent to the interventional environment. Currently, we are only aware of a single system that uses vision based gesture recognition for computer aided interventions [182]. Dynamic face-based gestures are used to guide a robot holding a laparoscope, based on tracking of the location of the physicians' eyes or a marker on the surgical cap. To achieve robustness the physician faces the camera head on, and the camera is adjusted so that the physicians' face is at the image center. This approach alleviates most of difficulties associated with a general setup, and is possible because it does not deviate from the current surgical practice where the physician is facing a monitor head on. In addition, to ensure safety a priming gesture is required before command gestures are issued.

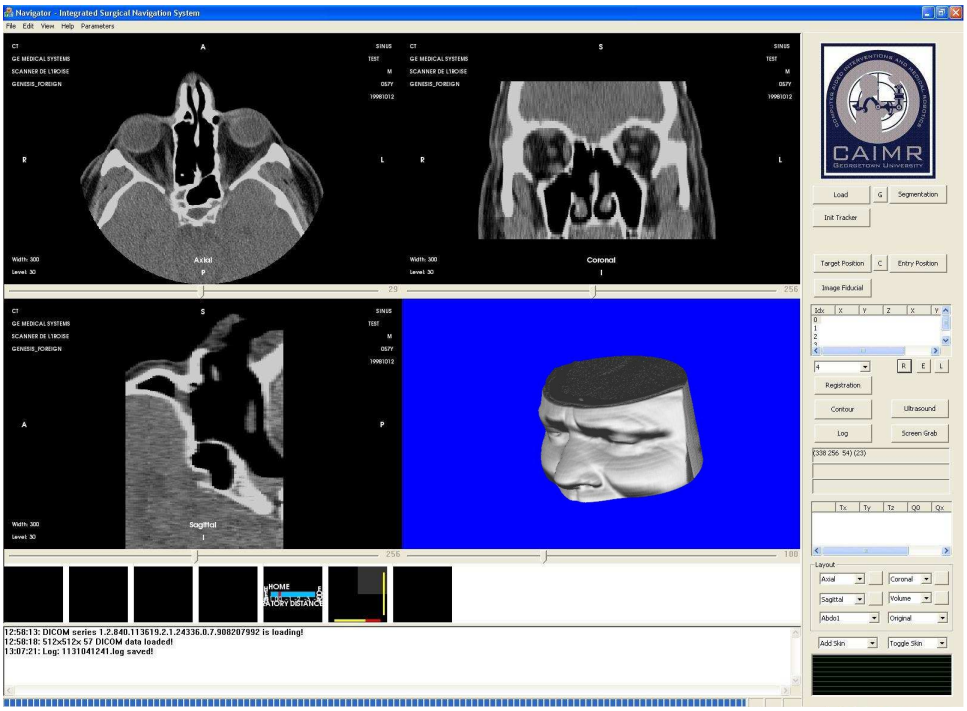

Figure 7: The common, quadrant based, IGP information display. Axial, sagittal, and coronal, views displayed head on and a 3D view.

Currently, the majority of IGP systems use standard computer monitors for display, and a four quadrant based data presentation. Three of the quadrants are used to display axial, sagittal and coronal views, and the fourth quadrant provides a 3D rendering of the anatomy (Figure 7). The main reasons for using this approach are that it is applicable to a wide variety of procedures and that physicians are used to these standard cross-sectional views. Other options for presenting the same information exist, with the most straightforward one displaying the axial, sagittal and coronal, views in their actual spatial locations as shown in Figure 8. A recent human factors study [251] determined that this combined 2D/3D information presentation is more effective than strict 2D or 3D guidance for non-experts performing spatial tasks. It is not clear if these results are directly applicable in the context of IGP as physicians are trained to infer spatial relationships based solely on 2D images.

The main disadvantage of this approach stems from the use of standard monitors as the display device. Information is displayed away from the interventional site, leading physicians to either divide their attention between the patient and display, or focus all their attention on the display. In the latter case, the physician is relying solely on tactile feedback to indicate that the displayed information is erroneous.

Several systems and devices for in-situ information display have been proposed. These include miniature LCD screens, stereo operating microscopes and binoculars, stereoscopic head mounted displays (HMD), and translucent displays. The main differences between these displays are in their level of obtrusiveness on current practice and their

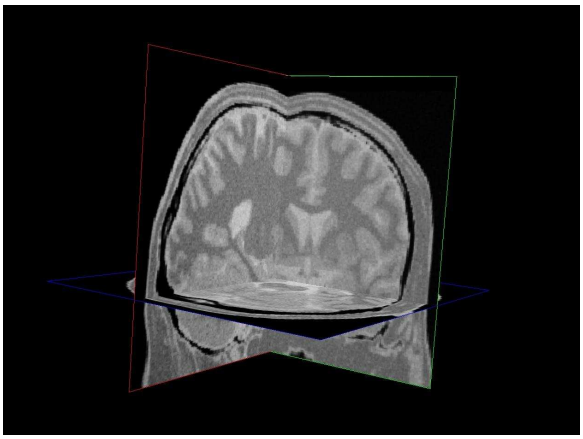

Figure 8: Axial, sagittal and coronal views displayed in their actual spatial locations.

system requirements (e.g. some require a tracking system).

Miniature LCD displays are a natural extension of the current display approach. Using a small screen allows the physician to place it next to the interventional site. Information is displayed either in a standard manner [152, 28], or when combined with a tracking system, according to the spatial relationship between display and patient [267] or tool and patient [152]. The main advantage of this approach arises from the use of a small screen which is also its main disadvantage. The amount of information that can be conveyed on the screen is limited. This is why these devices are usually used in conjunction with a standard display. Guidance information is usually conveyed via symbolic graphic representations (e.g. gauges, cross-hairs), although display of the image data is also possible.

Stereo augmented operating microscopes [57] and binoculars [19] overlay anatomical information onto the images viewed through the oculars. These are non-obtrusive augmented reality systems based on optical devices that are currently used in neurosurgical procedures. Internal anatomical structures are overlayed onto the optical images creating the illusion of a transparent object surface, with the goal of creating accurate depth perception. Unfortunately, depth perception is a subjective aspect of these systems and may not always be achievable [109]. Depth perception is effected by the choice of virtual object rendering method (e.g. wireframe, solid) and the real and virtual image composition method. In addition, non-subjective proximity queuing is possible by linking the rendering and composition methods to tool proximity [19]. An additional aspect of this approach is that it requires a tracking system, as the location and orientation of the patient and optical instrument must be known at all times.

Stereoscopic head mounted displays provide similar functionality and have been proposed for procedures where the physician currently uses a standard monitor to view interventional images. These type of systems have been developed for ultrasound guided biopsies [214, 123], and laparoscopic procedures [73]. Images from a pair of video cameras that are built into the head mounted display are overlayed with rendered images of the

system type	medical imaging and image processing	data visualization	segmentation	registration	tracking systems	HCI
Tomographic image overlay systems	√	√				√
Fluoroscopic X-ray systems	√	√			√	√
CT/MR based systems	√	√	√	√	√	√
Video based augmented reality systems	√	√	√	√	√	√

Table 3: Reviewed IGP systems and the technical components they incorporate.

internal anatomical structures, and the composite image is displayed. Unlike operating microscopes and binoculars, head mounted displays are intrusive, significantly changing current medical practice. This is why these systems need to provide a significant benefit if they are to be adopted as an in-situ display method. In addition, these systems also require tracking of the patient and HMD poses.

Translucent displays utilize semi-transparent mirrors to enable simultaneous viewing of patient and internal anatomical structures. Images of the internal structures are displayed on a monitor such that their reflection in a semi-transparent mirror coincides with the patient location as viewed through it. Two types of systems utilizing this approach have been proposed: a system using volumetric information and stereo to create depth perception [23], and systems that show a single tomographic image at a time [234, 32, 155, 65]. The former system requires the physician to wear stereo glasses and uses a tracking system, so that the location of the patient and the physician's eyes are known at all times. This approach is rather intrusive, and the authors conclude that a better design would be akin to a surgical microscope, similar to the the systems described above. The latter type of system employ a single image at a time, creating the illusion that the CT slice [155, 65], MR slice [67], or ultrasound image [234, 32] are floating inside the patient, coincident with the imaging plane. Although this approach does not provide depth perception, it is applicable to a large number of procedures, mainly needle based, where in-plane views are sufficient. This approach is relatively non-intrusive and does not require tracking which makes it particulary attractive cost wise.

4 Systems

The following sections review existing IGP systems in order of increasing complexity, where complexity is defined as the number of technical elements incorporated into the system. Table 3 presents the reviewed IGP systems and the technical components they incorporate. An interesting aspect of IGP is that increasing complexity does not coincide with the chronological order of appearance. Most notably video-based augmented reality, preceded both tomographic image overlay and fluoroscopic X-ray systems, both of which are less complex systems.

4.1 Tomographic image overlay systems (navigation using 2D tomographic images)

Tomographic image overlay systems provide guidance using a novel image display approach incorporating semi-transparent mirrors. These are research systems which are currently not available commercially. This approach has been used for real-time display of US images as described in [234] and for display of CT [65] and MR [67] images as shown in Figure 9. A monitor and a semi-transparent mirror are positioned so that when the physician views the patient through the mirror the reflection of the image from the monitor appears to float inside the patient. These systems are most suitable for needle based procedures where navigation on a single tomographic slice is sufficient.

System operation involves a single calibration step where the scaling and orientation parameters of the displayed image are computed so that its reflection in the mirror is physically accurate. Calibration is valid as long as the relationship between the mirror, monitor, and imaging device (US probe or CT gantry) is fixed. Intrinsic system accuracy is only dependent on the geometric accuracy of the images and the accuracy of the calibration procedure. The systems are low cost and relatively unobtrusive, with all hardware mounted directly onto the imaging devices. The procedure workflow remains the same, with no additional system related requirements (Figure 10).

Tomographic image overlay systems can potentially lead to improved outcomes in many needle based interventions since these systems bridge the perceptual discontinuity between the patient and the imaging monitor present in current practice. With this new approach the physician's attention is focused only on the interventional site, and there is no need to alternate between the screen and the patient.

4.2 Fluoroscopic X-ray systems (navigation using 2D projective images)

Fluoroscopic X-ray systems, also known as virtual fluoroscopy, replace the frequent use of C-arm fluoroscopic X-ray imaging with a fixed set of X-ray images and dynamic, real-time, projections of tool representations onto the images [71, 99]. An example screenshot from the Medtronic system is shown in Figure 11. This approach is equivalent to continuous imaging from multiple directions without the radiation. As no pre-operative imaging is involved these systems are primarily used for procedures that involve only qualitative planning, or when immediate intervention is required (i.e. trauma). In addition, all objects are assumed to be rigid and are either dynamically tracked using optical tracking or immobilized. These systems were readily accepted by the orthopedics community as their workflow only deviates slightly from current practice, requiring minimal training.

The system workflow is presented in Figure 12 and is as follows. Intra-operatively a calibration target is mounted to the image intensifier of the C-arm. All surgical tools and the C-arm are fitted with dynamic reference frames, with the C-arm's reference

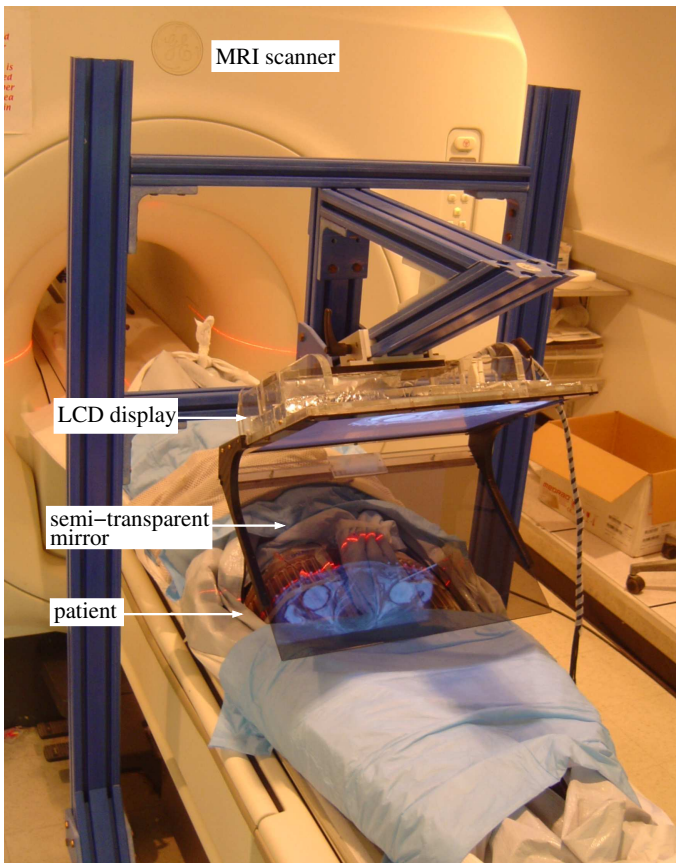

Figure 9: MR based tomographic image overlay guidance system (courtesy G. Fichtinger).

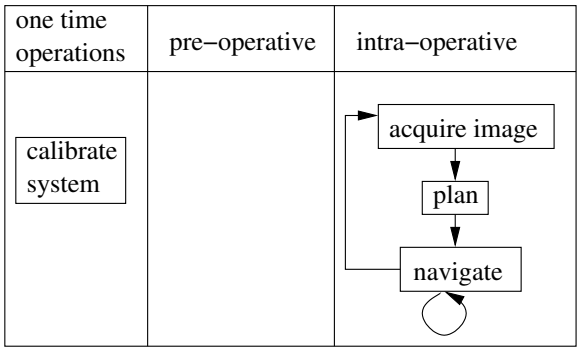

Figure 10: Workflow for tomographic image overlay navigation systems.

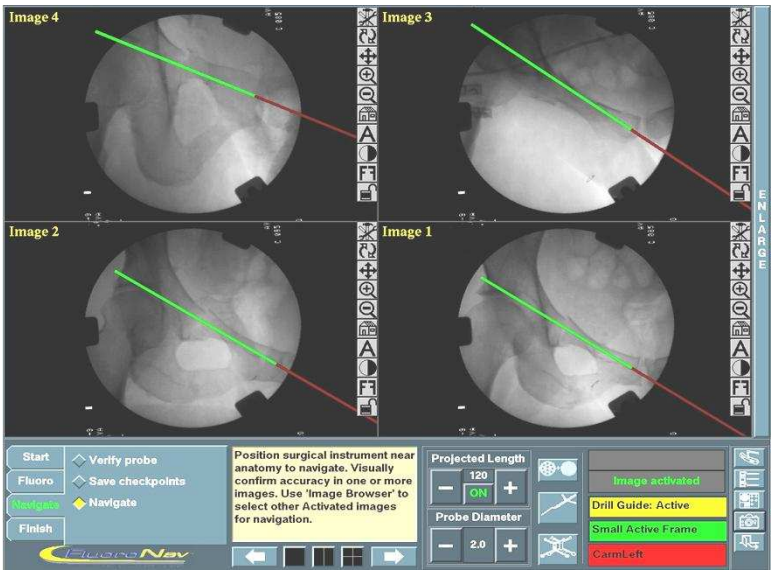

Figure 11: Screenshot of the Medtronic Fluoronav® virtual fluoroscopy system. A tool and its virtual extension are projected onto the image set.

frame usually incorporated into the calibration target structure. The anatomy is either fitted with a reference frame or immobilized. The optical tracking system is positioned appropriately to accommodate the line of site restriction. The tools are then calibrated, that is, the rigid transformation between the tool coordinate system and the dynamic reference frame is estimated. Fluoroscopic images of the anatomy are acquired and the C-arm is calibrated for each image, estimating image distortions and projection parameters. The physician then formulates a surgical plan from the images and carries it out with the aid of the system. The tools are dynamically tracked and projected onto the images. When the relationship between anatomical structures changes new images can be acquired and the plan modified accordingly.

The potential benefits of this type of system are threefold: (1) improved outcomes in existing interventions; (2) reduced radiation exposure; and (3) enabling new types of interventions. Improved outcomes are possible as the system replaces intermittent guidance based on X-ray images with continuous multi-view guidance. Radiation exposure to the patient and physician is lowered as the number of acquired X-ray images is considerably less than in current practice. Finally, new percutaneous interventions that were previously considered impractical due to the expected amount of imaging are now possible, as the system provides continuous radiation-free guidance.

The main disadvantages of this approach are twofold: it is somewhat obtrusive, and the guidance is based on 2D images. The use of optical tracking may require the O.R. staff to modify their behavior so that an unobstructed line of sight between the tracked instruments and the tracking system's cameras is always available. Additionally, as guidance is based on 2D X-ray images the physician has to mentally reconstruct the underlying 3D anatomical structures, which is a hard task.

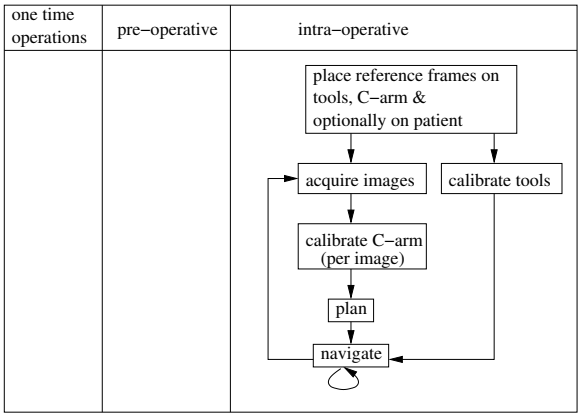

Figure 12: Workflow for virtual fluoroscopy navigation systems.

Virtual fluoroscopy systems are currently available from several commercial vendors and have been applied mainly in the field of orthopedics. Example applications include femoral neck fractures [113], femoral and tibial shaft fractures [236, 94], pelvic fractures [174], total knee arthroplasty [260], spinal surgery [75, 101, 183], and removal of gunshot and shrapnel [175].

4.3 CT and MR based systems (navigation using 3D images)

CT and MR-based systems replace the use of stereotactic frames with dynamic, real-time, three-dimensional views of anatomical structures and surgical tools. These systems require that all tools be fitted with reference frames so that they can be tracked in real-time, with the exception of endoscopic systems that use ego-motion tracking (see section 3.5). Anatomical structures are either fitted with a dynamic reference frame and tracked, or immobilized. Most systems display the information using the quadrant view as described in section 3.6, although surface rendered structures in conjunction with volume re-slicing may be a more appropriate visualization technique for specific procedures [212]. These systems are commercially available for procedures involving rigid anatomical structures. Several research systems extend this ability to deal with deformations such as those exhibited by brain shift. These extensions replace rigid registration with deformable registration (see section 3.4) and usually assume that once the brain is registered it is stationary, although in practice brain pulsation (motion due to the cardiac cycle) is always present [62]. This approach has been extended to deformable and non-stationary structures in [22], which deals with motion and deformation of the liver throughout the respiratory cycle.

The potential benefits of this type of system are similar to those of virtual fluoroscopy: improved outcomes in existing interventions, reduced radiation exposure in procedures that use intra-operative X-ray imaging, and enabling new types of interventions by providing accurate guidance that is currently not available via intra-operative imaging.

The main disadvantages of this approach are that it requires the acquisition of a volu-

metric data set which in current practice is not always acquired, and that the workflow deviates significantly from conventional practice.

We divide CT/MR systems into four main subcategories according to the registration method used: (1) contact fiducial-based; (2) contact anatomy-based; (3) image based; and (4) no registration. Systems that employ various combinations of fiducials, anatomical landmarks, and images for registration exist, but are not reviewed herein.

CT/MR systems, contact fiducial-based registration

CT and MR-based systems utilizing contact fiducial-based registration have been in use for over a decade. These systems usually incorporate all of the IGP components reviewed above: imaging, visualization, segmentation, registration, tracking, and user interaction. A typical system workflow is presented in Figure 13(a) and is as follows. Pre-operatively fiducials are placed on the patient and a volumetric data set is acquired. The choice of fiducial type is based upon the required registration accuracy. High risk procedures usually use invasive fiducials that are surgically fixed to the anatomical structure, while lower risk procedures that can accommodate larger registration errors may use adhesive skin markers. Once the volumetric data set is acquired a plan is formulated by the physician. This may require segmentation of the data, or more often the segmentation is implicit. Finally, fiducial locations in the volumetric data set are identified, either manually or semi-automatically. Intra-operatively, the tracking system is positioned in place and the tools are fitted with reference frames, and calibrated. The anatomy is either fitted with a reference frame or possibly immobilized. Fiducial locations are identified and matched with their location in the volumetric data set. Identification of fiducial location is done by touching a tracked calibrated probe to each fiducial or in some cases the tracking system can automatically identify the fiducials. Once the pre-operative and intra-operative fiducial locations are known, paired point registration is performed. All tool and anatomical structure locations are then transferred to the same coordinate system and displayed on screen. During the procedure the display is continuously updated based on the tracked tools and anatomy locations.

These systems are available from several research laboratories and commercial vendors. They have been used in a variety of neurosurgical procedures [85, 160] including biopsies, tumor resections, skull based surgery, and more recently for deep brain stimulation [100]. In orthopedics these systems have been employed in a variety of procedures [53, 184] including pedicle screw insertion, total knee replacement, and total hip replacement. In maxillofacial surgery they have been applied to insertion of dental implants [20, 29, 30, 166], with the commercial systems providing automatic fiducial based registration, dispensing with manual intra-operative fiducial digitization. These systems have also been used in endoscopic sinus and spine surgeries [223, 158], and sinus and skull base surgeries [165, 187, 277].

CT/MR systems, contact anatomy-based registration

CT and MR based systems utilizing contact anatomy-based registration are an immediate extension of fiducial-based systems. Fiducials are replaced with anatomical landmarks and a surface representation of the anatomy. The system workflow is pre-

sented in Figure 13(b) and is as follows. Pre-operatively, a volumetric data set is acquired. The surface of the anatomical structure is then segmented from this data and anatomical landmarks are identified. The procedure is then planned by the physician. Intra-operatively, the workflow proceeds as outlined above with the only difference being that the physician digitizes the anatomical landmarks and surface points instead of the fiducials. Paired point registration using the anatomical landmarks serves as an initial transformation estimate for iterative estimation based on the digitized surface points. While this approach is less invasive than surgically placed fiducials it is highly dependent on the accuracy of the segmentation, point acquisition and the registration algorithm. Once registration is performed the procedure proceeds exactly as described above.

These systems are also available from several research laboratories and from commercial vendors. They have been used in a variety of orthopedic procedures including total hip replacement [274], total knee arthroplasty [10], distal radius osteotomy [45], periacetabular osteotomy [159], and various spinal surgeries [33, 75, 101]. In ENT surgery these system have been used for sinus and skull base surgery [165, 187, 277]. More recently, this system type was applied to bronchoscopic biopsies of peripheral lung lesions [11], with airway bifurcations serving as anatomical landmarks.

CT/MR systems, image based registration

CT/MR based systems utilizing image-based registration provide non-invasive registration, replacing contact based point acquisitions with images of the anatomical structures. This approach is potentially faster than the previous registration approaches, replacing repeated manual point acquisition with image acquisition. In addition it is less variable and prone to human-error as it does not involve manual acquisition of anatomical landmarks and surface points which are physician dependent [211].

The system workflow is presented in Figure 13(c) and is as follows. Pre-operatively, a volumetric data set is acquired. Depending upon the registration approach, intensity, geometry or hybrid, features are extracted from the data. These can be the anatomical surfaces, volume gradients or the original intensities (see section 3.4). The procedure is then planned by the physician. Intra-operatively, the workflow proceeds as outlined for contact fiducial-based systems where fiducial digitization is replaced by camera calibration and image acquisition. The camera is either calibrated once or in the case of fluoroscopic X-rays it is calibrated per-image. Images of the anatomical structure are then acquired and depending upon the registration approach features are extracted. Again these are contours, gradients or the original intensities. Finally, the pre-operative image data is registered to the intra-operative data. Once registration is performed the procedure proceeds exactly as in the previously described systems.

These systems are available from several research laboratories and have only recently been commercialized. The commercial products are primarily targeted towards spine surgery, registering pre-operative CT images using intra-operative fluoroscopic X-rays [50], although they have also been used for hip surgery [90]. Endoscopic systems that utilize this approach have been reported in [26] and [170, 171]. Currently, these are research systems that have not been used in clinical practice.

CT/MR systems, no registration

CT/MR based systems that do not require registration are based on the acquisition of intra-operative volumetric data sets. The imaging modalities are either interventional MRI or C-arm CT's. The images, patient, and tracking system are intrinsically registered, as the relationship between the tracking and imaging systems is known. This approach reduces the operating time as registration is immediate. In addition, updated volumetric data sets can be acquired throughout the procedure, reflecting changes in the anatomical structures. This approach has two main deficiencies: image quality is lower than that of diagnostic CT and MR machines, and there is no transfer of a quantitative pre-operative plan to the intra-operative stage (i.e. no registration). This is why this approach is most suitable for procedures that do not require extensive planning.

The system workflow is presented in Figure 13(d) and is as follows. Intra-operatively, tools are fitted with reference frames and calibrated. The anatomy is either fitted with a reference frame or possibly immobilized. Volumetric images are acquired and the physician formulates a plan and acts upon it. As no explicit registration is acquired the physician can immediately start navigating. If at any time during the procedure the physician judges that the images no longer accurately represent the intra-operative situation, new images are acquired.

These systems are available from several research laboratories and from commercial vendors. They have mainly been used in neurosurgery and orthopedics for a variety of procedures including, brain biopsies [172], craniotomies [88], and surgical procedures in the pelvis [86], talus [86, 207], and spine [75, 86, 101, 104, 261]. Initial evaluations of the C-arm CT based approach for ENT surgery have recently been reported in [255] and [198].

4.4 Video based augmented reality systems (navigation using 2D projective images)

Video-based augmented reality systems provide guidance by overlaying the video imagery with information about the anatomical structures and tools that are underneath the visible surface. These systems require that all tools be fitted with reference frames so that they can be tracked in real-time. Anatomical structures are either fitted with a dynamic reference frame and tracked, or immobilized. These systems combine all the technical aspects of virtual fluoroscopy systems and MR/CT based systems. Most notably, navigation is based on 2D projective images, similar to virtual fluoroscopy, but registration is a requirement, similar to CT/MR based systems. Information is displayed either on a screen or directly into an optical device used to view the anatomy. The display used is closely tied to current medical practice. If the anatomy is already viewed through an optical device (e.g. operating microscope), then injecting the additional information into the field of view is natural. If, on the other hand, the anatomy is viewed directly, either a head-mounted display or a screen is used. As navigation is based on 2D projective images, conveying depth information is an issue. If the images are displayed

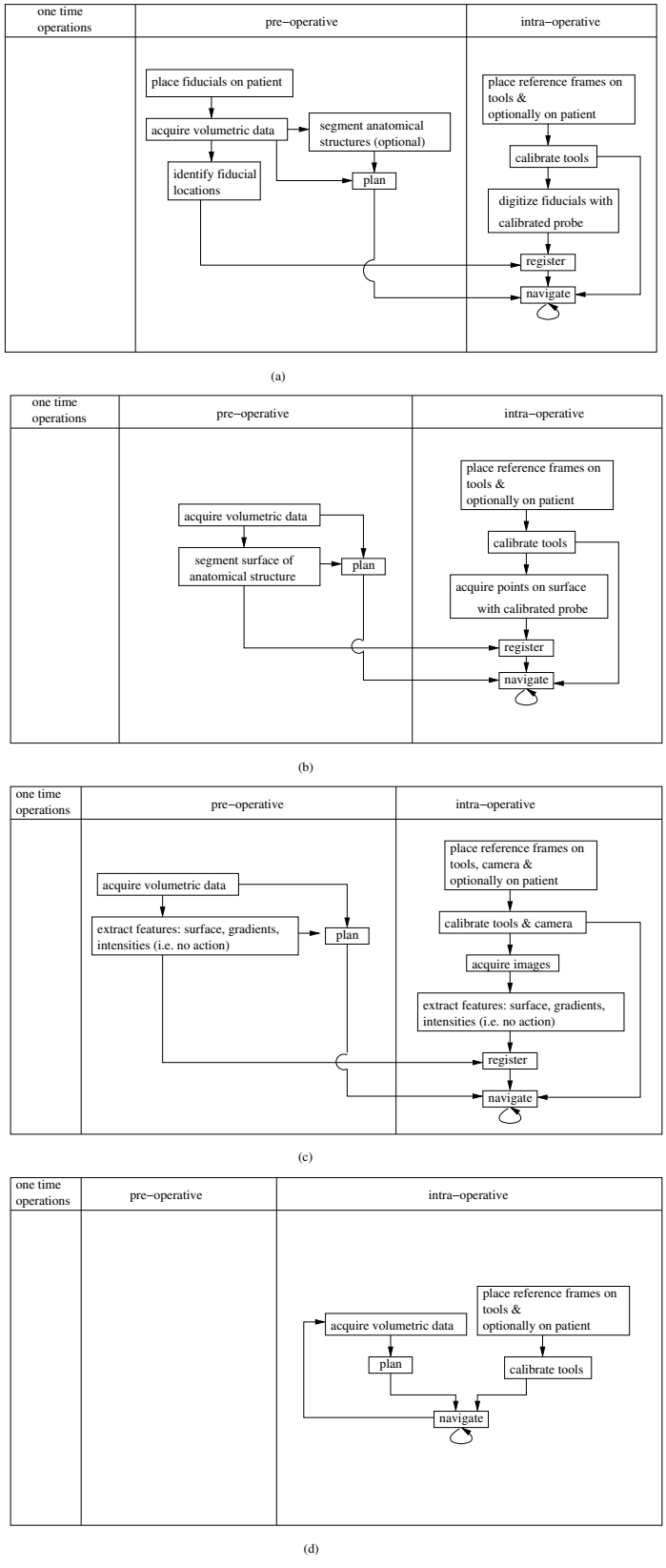

Figure 13: Workflow for CT/MR navigation systems (a) contact fiducial-based registration (b) contact anatomy-based registration (c) image-based registration (d) no registration.

on a standard screen, all depth information is implicit and the physician must mentally recreate the underlying spatial structures. If images are displayed stereoscopically depth information is available explicitly.

The system workflow is a combination of the workflows for fluoroscopic X-ray systems and CT/MR based systems. We limit our description here to systems employing contact fiducial-based registration. All other registration approaches used by CT/MR systems are also applicable, leading to similar workflow combinations. Figure 14 presents the workflow which is described next. Pre-operatively, fiducials are placed on the patient and a volumetric data set is acquired. The volume is segmented and the physician formulates a plan. Finally, fiducial locations in the volumetric data set are identified. Intra-operatively, the tracking system is positioned in place and the tools and cameras are fitted with reference frames. The anatomy is either fitted with a reference frame or possibly immobilized. Fiducials are digitized by touching them with a calibrated probe, paired with their location in the volumetric data set, and the rigid transformation is computed. Up to this point, the workflow is the same as a CT/MR based system, and from this point the workflow mimics a fluoroscopic X-ray system. The cameras are now calibrated and navigation can begin. Tools, cameras, and anatomical structures can freely move relative to each other as they are continuously tracked. Video images are acquired continuously and representations of the anatomical structures and tools are projected onto them. These are usually surface models of anatomical structures and tools that are projected onto the images either as semi-transparent, wire-frame, or opaque objects.

The potential benefits of this type of system are similar to those of the previous systems: improved outcomes in existing interventions, and enabling new types of interventions by providing accurate guidance that is currently not available via intra-operative imaging.

This approach has several disadvantages, most noticeably, conventional procedure workflow changes considerably, requiring both calibration of optical devices and registration of anatomical structures. Additional disadvantages stem from the use of projective images for navigation and the different approaches to their display. Systems that inject information into the field of view of an optical device are either limited to procedures that already use the device (e.g. operating binoculars) or require the introduction of an optical device (e.g. head mounted display) which may be considered too obtrusive. On the other hand, systems that display images using a standard screen do not provide explicit depth information of the overlayed structures.

These systems are available from several research laboratories, but have not transitioned into commercial products. Systems utilizing stereoscopic displays have been developed for breast biopsies [214], and for neurosurgical procedures [19, 66, 57]. Systems utilizing screen-based display have been developed for neurosurgical procedures [84] and more recently for radio frequency ablation of liver tumors [180, 181].

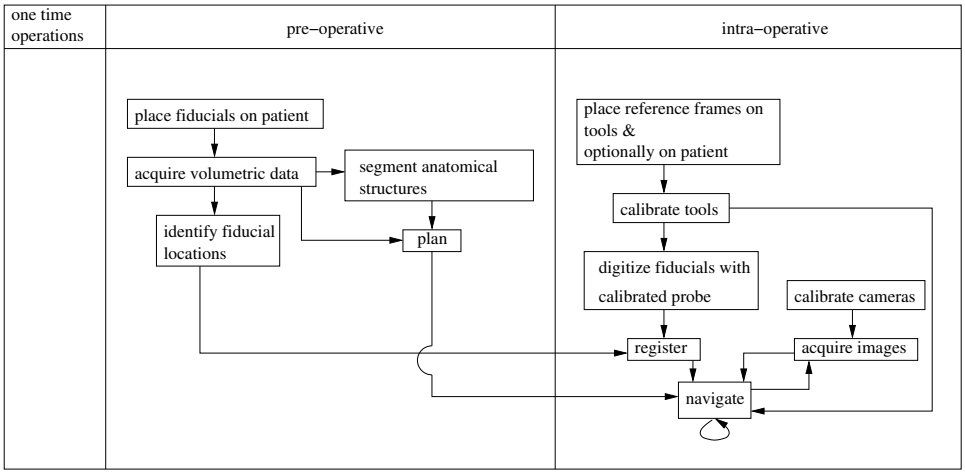

Figure 14: Workflow for video based augmented reality systems using fiducial-contact based registration. Similar to CT/MR systems, workflow will vary depending on the employed registration approach: contact fiducial, contact anatomy, image-based, and no registration.

5 Discussion

From this review it is clear that current IGP systems still assume that anatomical structures are rigid objects, perhaps with the exception of systems that compensate for brain shift. While this is a limitation, in practice there are many procedures where this assumption is valid. Another, less obvious limitation has to do with the display of the anatomical structures. Systems that treat images as a single object, deferring the task of segmentation to the physician, are not only limited to rigid motion but also assume that all anatomical structures have the same motion. If during the procedure the relative pose of the structures changes the images are no longer valid. Example systems exhibiting this behavior are CT/MR systems which use image re-slicing as their display method and fluoroscopic X-ray systems. Overcoming this limitation requires either segmentation of the images, enabling independent rendering of separate anatomical structures, or continuously acquiring updated images. The later solution is not optimal if the imaging involves ionizing radiation which is the case with fluoroscopic X-ray systems. Ad-hoc solutions to this problem exist such as selective use of the guidance information, ignoring parts of the image data which are known to have changed [176], but more generally applicable solutions are needed.

Among the systems described above the most successful and widely used are CT/MR systems using contact anatomy and fiducial based registration and fluoroscopic X-ray systems. To understand why these specific systems have gained acceptance we look at their use of the technologies described in section 3.

The imaging required by both systems is the same as in current practice. Data visualization in CT/MR systems is done by surface rendering and volume re-slicing which are the simplest forms of visualization. In the case of fluoroscopic X-ray systems the

images are displayed exactly as in current practice, with the only difference being that they are automatically corrected for geometric distortion. Segmentation in CT/MR systems is usually limited to bone surfaces extracted via thresholding and is performed pre-operatively. Fluoroscopic X-ray systems do not incorporate segmentation. Registration in CT/MR systems is performed by digitizing anatomical landmarks and surface points using a tracked calibrated probe and rigidly aligning them to the segmented surface. Fluoroscopic X-ray systems are registration-less. Tracking in both systems types is usually based on optical systems and rigid tools and anatomical structures. Finally, interaction with both system types is based on the use of touch screens, foot pedals, or a virtual keyboard. Information is displayed on standard screens with CT/MR systems using conventional axial, sagittal, and coronal views with an additional 3D view with tools displayed in each of the views. Fluoroscopic X-ray systems display the images exactly as in conventional fluoroscopy with the tracked tools projected onto the images.

From the preceding paragraph it is clear that the main reasons for the acceptance of these specific systems is that their workflow and behavior are close to current clinical practice. Technically they employ mature technologies, using the simplest possible solutions. The workflow is constrained so that the number of possible actions at any step during the procedure is limited. Finally, the intra-operative overhead of using these systems is minimal. Setting up the system only involves positioning the tracking system and mounting dynamic reference frames onto tools and anatomical structures. In the case of contact-based CT/MR systems there is also an additional registration step which can still be a bottleneck in the procedure flow, as the physicians repeatedly perform registration until the resulting error is sufficient for their purposes. We expect this problem will be solved in the near future using image-based registration methods that are robust and fast enough for intra-operative use.

Currently, IGP research is turning its focus to procedures involving soft tissue, departing from the rigid body assumption. These procedures deal with structures that can deform between the different procedure steps (e.g. prostate), or throughout them (e.g. liver). Continuous deformations throughout a procedure usually arise from the cyclic respiratory and cardiac motions. One growing area of research that aims at addressing this is the development of patient specific models of organ motion and deformation.

This departure from the rigid body assumption effects most components of the IGP systems. Volumetric imaging needs to be extended to incorporate time, yielding 4D data sets. As volumetric data sets are acquired using a slice based approach, accounting for deformations due to respiratory/cardiac motion is based on monitoring these signals. Images are either acquired in a gated manner [275] or retrospectively sorted according to their location in the respiratory/cardiac cycle [121]. Intra-operatively one suitable modality for soft tissue imaging is US or real-time 3D-US, which is now becoming available. As this modality is real-time and non-ionizing it is suitable for continuous monitoring. Visualization can be performed using currently available techniques to render the time varying volumetric data, although direct volume rendering methods will probably not provide sufficient rendering rates. Segmentation of these sets of volumes using a fully manual approach is not an option. On the other hand formulating segmen-

tation as a registration task for this type of data is natural. One volumetric data set is segmented, possibly manually, and this segmentation is propagated to the other volumes via registration. Registration needs include the development of fast deformable registration algorithms. When dealing with stationary anatomical structures that only deform between procedure steps faster variants of current deformable registration methods may suffice, but this is not the case when the motion and deformations are continuous. In this case registration and tracking are intertwined. Determining the location and shape of the anatomical structures based solely on currently available intra-operative information is an ill-posed problem. Additional constraints derived from patient specific models of motion and deformation are needed. This model-based approach has been recently used to estimate internal tumor motion based on skin marker tracking and intermittent X-ray imaging [222], and for assessing the motion and deformation of the liver using US imaging [22].

Finally, as the motivation underlying the development of IGP systems is to provide better healthcare it seems appropriate to look at the impact of IGP systems on current medical practice. At this time it is still not clear. Most clinical studies tend to favor IGP systems over the traditional approach as described in [55, 200, 206]. They conclude that IGP systems provide better or equivalent accuracy to that found in current practice, in addition to reducing radiation exposure in procedures that employ X-ray imaging. On the other hand some studies [230] conclude that while the accuracy of IGP systems is equivalent to conventional practice, their cost related overhead is too high. Therefore, it is important for IGP researchers to work closely with clinical partners to ensure the technology we develop will ultimately benefit patient care.

References

[1] *Health Risks From Exposure To Low Levels Of Ionizing Radiation.* The National Academies Press, 2005.

[2] N. Ahuja and M. H. Yang. *Face Detection and Gesture Recognition for Human-Computer Interaction.* Kluwer, 2001.

[3] K. S. Arun, T. S. Huang, and S. D. Blostein. Least-squares fitting of two 3-D point sets. *IEEE Trans. Pattern Anal. Machine Intell.*, 9(5):698–700, 1987.

[4] K. Vijayan Asari, Sanjiv Kumar, and D. Radhakrishnan. A new approach for nonlinear distortion correction in endoscopic images based on least squares estimation. *IEEE Trans. Med. Imag.*, 18(4):345–354, 1999.

[5] Michel A. Audette, Kaleem Siddiqi, Frank P. Ferrie, and Terry M. Peters. An integrated range-sensing, segmentation and registration framework for the characterization of intra-surgical brain deformations in image-guided surgery. *Computer Vision and Image Understanding*, 89:226–251, 2003.

[6] Nicholas Ayache, Philippe Cinquin, Isaac Cohen, Laurent Cohen, François Leitner, and Olivier Monga. Segmentation of complex three-dimensional medical objects: A challange and a requirement for computer-assisted surgery planning and performance. In R. H. Taylor, S. Lavallée, G. C. Burdea, and R. Mösges, editors, *Computer-integrated surgery, Technology and clinical applications*, chapter 4, pages 59–74. MIT Press, Cambridge Ma., 1995.

[7] Filip Banovac et al. Liver tumor biopsy in a respiring phantom with the assistance of a novel electromagnetic navigation device. In *Medical Image Computing and Computer-Assisted Intervention*, pages 200–207, 2002.

[8] Ravi Bansal, Lawrence H. Staib, Zhe Chen, Anand Rangarajan, Jonathan Knisely, Ravinder Nath, and James S. Duncan. Entropy-based, dual-portal-to-3DCT registration incorporating pixel correlation. *IEEE Trans. Med. Imag.*, 22(1):29–49, 2003.

[9] Ravi Bansal, Lawrence H. Staib, and Bradley S. Peterson. Correcting nonuniformities in MRI intensities using entropy minimization based on an elastic model. In *Medical Image Computing and Computer-Assisted Intervention*, pages 78–86, 2004.

[10] H. Bäthis, L. Perlick, M. Tingart, C. Lüring, C. Perlick, and J. Grifka. Radiological results of image-based and non-image-based computer-assisted total knee arthroplasty. *Int. Orthop.*, 28(2):87–90, 2004.

[11] Heinrich Becker, Felix Herth, Armin Ernst, and Yehuda Schwarz. Bronchoscopic biopsy of peripheral lung lesions under electromagnetic guidance: A pilot study. *Journal of Bronchology*, 12(1):9–13, 2005.

[12] Greg Bednarz et al. Evaluation of the spatial accuracy of magnetic resonance imaging-based stereotactic target localization for gamma knife radiosurgery of functional disorders. *Neurosurgery*, 5(5):1156, 1999.

[13] Gert Behiels, Frederik Maes, Dirk Vandermeulen, and Paul Suetens. Evaluation of image features and search strategies for segmentation of bone structures in radiographs using active shape models. *Medical Image Analysis*, 6(1):47–62, 2002.

[14] Said Benameur, Max Mignotte, Stefan Parent, Hubert Labelle, Wafa Skalli, and Jacques de Guise. 3D/2D registration and segmentation of scoliotic vertebrae using statistical models. *Comput. Med. Imaging Graph.*, 27(5):321–337, 2003.

[15] Paul J. Besl and Neil D. McKay. A method for registration of 3D shapes. *IEEE Trans. Pattern Anal. Machine Intell.*, 14(2):239–255, 1992.

[16] J. Bijhold. Three-dimensional verification of patient placement during radiotherapy using portal images. *Med. Phys.*, 20(2):347–356, 1993.

[17] W. Birkfellner et al. Systematic distortions in magnetic position digitizers. *Med. Phys.*, 25(11):2242–2248, 1998.

[18] Wolfgang Birkfellner et al. Calibration of tracking systems in a surgical environment. *IEEE Trans. Med. Imag.*, 17(5):737–742, 1998.

[19] Wolfgang Birkfellner et al. Computer-enhanced stereoscopic vision in a head-mounted operating binocular. *Phys. Med. Biol.*, 48:49–57, 2003.

[20] Wolfgang Birkfellner, Klaus Huber, Alan Larson, Dennis Hanson, Markus Diemling, Peter Homolka, and Helmar Bergmann. A modular software system for computer-aided surgery and its first application in oral implantology. *IEEE Trans. Med. Imag.*, 19(6):616–620, 2000.

[21] P.M. Black et al. Development and implementation of intraoperative magnetic resonance imaging and its neurosurgical applications. *Neurosurgery*, 41(4):831–842, 1997.

[22] Jane M. Blackall, Graeme P. Penney, Andrew P. King, and David J. Hawkes. Alignment of sparse freehand 3-D ultrasound with preoperative images of the liver using models of respiratory motion and deformation. *IEEE Trans. Med. Imag.*, 24(11):1405–1416, 2005.

[23] Mike Blackwell, Constantinos Nikou, Anthony M. DiGioia, and Takeo Kanade. An image overlay system for medical data visualization. *Medical Image Analysis*, 4(1):67–72, 2000.

[24] C. Brack, R. Burgkart, A. Czopf, and H. Götte. Accurate X-ray-based navigation in computer-assisted orhopedic surgery. In *Computer Assisted Radiology and Surgery*, 1998.

[25] Elizabeth Bullitt and Stephen R. Aylward. Volume rendering of segmented image objects. *IEEE Trans. Med. Imag.*, 21(8):998–1002, 2002.

[26] Darius Burschka, Ming Li, Masaru Ishii, Russell H. Taylor, and Gregory D. Hager. Scale-invariant registration of monocular endoscopic images to ct-scans for sinus surgery. *Medical Image Analysis*, 9(5):413–426, 2005.

[27] Brian Cabral, Nancy Cam, and Jim Foran. Accelerated volume rendering and tomographic reconstruction using texture mapping hardware. In *VVS '94: Proceedings of the 1994 symposium on Volume visualization*, pages 91–98, 1994.

[28] M. A. Cardin, J. X. Wang, and D. B. Plewes. A method to evaluate human spatial coordination interfaces for computer-assisted surgery. In *Medical Image Computing and Computer-Assisted Intervention*, pages 9–16, 2005.

[29] Nardy Casap, Alon Wexler, Nathan Persky, Amir Schneider, and Joshua Lustmann. Navigation surgery for dental implants: Assessment of accuracy of the image guided implantology system. *J. Oral Maxillofac. Surg.*, 62:116–119, 2004.

[30] Nardy Casap, Alon Wexler, and Eyal Tarazi. Application of a surgical navigation system for implant surgery in a deficient alveolar ridge postexcision of an odontogenic myxoma. *J. Oral Maxillofac. Surg.*, 63:J Oral Maxillofac Surg 63:982–988, 2005, 2005.

[31] Matthieu Chabanas, Vincent Luboz, and Yohan Payan. Patient specific finite element model of the face soft tissues for computer-assisted maxillofacial surgery. *Medical Image Analysis*, 7(2):131–151, 2003.

[32] Wilson M. Chang, Michael B. Horowitz, and George D. Stetten. Intuitive intraoperative ultrasound guidance using the sonic flashlight, a novel ultrasound display system. *Neurosurgery*, 56:ONS 434–437, 2005.

[33] E. Thomas Chappell, Laura Pare, Matthew O. Dolich, Michael E. Lekawa, and Mohammed Salepour. Frameless stereotaxy to facilitate anterolateral thoracolumbar surgery: technique. *Neurosurgery*, 56(1):Suppl. 110–116, 2005.

[34] E. Chen, R. E. Ellis, and J. T. Bryant. A strain-energy model of passive knee kinematics for the study of surgical implantation strategies. In *Medical Image Computing and Computer-Assisted Intervention*, pages 1086–1095, 2000.

[35] Yang Chen and Gérard Medioni. Object modelling by registration of multiple range images. *Image and Vision Computing*, 10(3):145–155, 1992.

[36] Dmitry Chetverikov, Dmitry Stepanov, and Pavel Krsek. Robust Euclidean alignment of 3D point sets: the trimmed iterative closest point algorithm. *Image and Vision Computing*, 23(3):299–309, 2005.

[37] Gary E. Christensen, Sarang C. Joshi, and Michael I. Miller. Volumetric transformation of brain anatomy. *IEEE Trans. Med. Imag.*, 16(6):864–877, 1997.

[38] Adrian J. Chung, Philip J. Edwards, Fani Deligianni, and Guang Zhong Yang. Freehand co-calibration of an optical and electromagnetic tracker. In *Second International Workshop: Medical Imaging and Augmented Reality*, pages 320–328, 2004.

[39] Olivier Clatz, Hervé Delingette, Ion-Florin Talos, Alexandra J. Golby, Ron Kikinis, Ferenc A. Jolesz, Nicholas Ayache, and Simon K. Warfield. Robust non-rigid registration to capture brain shift from intra-operative MRI. *IEEE Trans. Med. Imag.*, 24(11):1417–1427, 2005.

[40] Kevin Cleary and Charles Nguyen. State of the art in surgical robotics: clinical applications and technology challenges. *Computer Aided Surgery*, 6(6):312–328, 2001.

[41] Roch M. Comeau, Abbas F. Sadikot, Aaron Fenster, and Terry M. Peters. Intraoperative ultrasound for guidance and tissue shift correction in image-guided neurosurgery. *Med. Phys.*, 27(4):787–800, 2000.

[42] T. F. Cootes, C. J. Taylor, D. H. Cooper, and J. Graham. Active shape models - their training and application. *Computer Vision and Image Understanding*, 60(1):38–59, 1995.

[43] Timothy F. Cootes, Gareth J. Edwards, and Christopher J. Taylor. Active appearance models. *IEEE Trans. Pattern Anal. Machine Intell.*, 23(6):681–685, 2001.

[44] Timothy F. Cootes, Andrew Hill, Christopher J. Taylor, and J. Haslam. Use of active shape models for locating structures in medical images. *Image Vision Comput.*, 12(6):355–365, 1994.

[45] H. Croitoru, R. E. Ellis, R. Prihar, C. F. Small, and D. R. Pichora. Fixation-based surgery:a new technique for distal radius osteotomy. *Computer Aided Surgery*, 6:160–169, 2001.

[46] John Danskin and Pat Hanrahan. Fast algorithms for volume ray tracing. In *VVS '92: Proceedings of the 1992 workshop on Volume visualization*, pages 91–98, 1992.

[47] Rhodri H. Davies, Carole J. Twining, Tim F. Cootes, John C. Waterton, and Chris. J. Taylor. A minimum description length approach to statistical shape modeling. *TMI*, 21(5):525–537, 2002.

[48] Benoit M. Dawant, S. L. Hartmann, Jean-Philippe Thirion, Frederik Maes, Dirk Vandermeulen, and P. Demaerel. Automatic 3D segmentation of internal structures on the head in MR images using a combination of similarity and free form transormations: Part I, metholody and validation on normal subjects. *IEEE Trans. Med. Imag.*, 18(10):909–916, 1999.

[49] P. Dawson. Patient dose in multislice CT: why is it increasing and does it matter? *The British Journal of Radiology*, 77:S10–13, 2004.

[50] H. Gordon Deen and Eric W. Nottmeier. Balloon kyphoplasty for treatment of sacral insufficiency fractures. report of three cases. *Neurosurg. Focus.*, 18(3):e7, 2005.

[51] Fani Deligianni, Adrian Chung, and Guang-Zhong Yang. Patient-specific bronchoscope simulation with pq-space-based 2d/3d registration. *Computer Aided Surgery*, 9(5/6):1–12, 2004.

[52] Maxime Descoteaux, Michel Audette, Kiyoyuki Chinzei, and Kaleem Siddiqi. Bone enhancement filtering: Application to sinus bone segmentation and simulation of pituitary surgery. In *Medical Image Computing and Computer-Assisted Intervention*, pages 9–16, 2005.

[53] Anthony DiGioia, Branislav Jaramaz, Frederick Picard, and Lutz Peter Nolte, editors. *Computer and Robotic Assisted Hip and Knee Surgery*. Oxford university press, 2004.

[54] Simon J. Doran, Liz Charles-Edwards, Stefan A. Reinsberg, and Martin O. Leach. A complete distortion correction for MR images: I. gradient warp correction. *Phys. Med. Biol.*, 50(7):1343–1361, 2005.

[55] N. L. Dorward, T. S. Paleologos, O. Alberti, and D. G. Thomas. The advantages of frameless stereotactic biopsy over frame-based biopsy. *British Journal of Neurosurgery*, 16(2):110–118, 2002.

[56] J. S. Duncan and N. Ayache. Medical image analysis: Progress over two decades and challenges ahead. *IEEE Trans. Pattern Anal. Machine Intell.*, 22(1):85–105, 2000.

[57] Philip J. Edwards et al. Design and evaluation of a system for microscope-assisted guided interventions (MAGI). *IEEE Trans. Med. Imag.*, 19(11):1082–1093, 2000.

[58] R. Fahrig, M. Moreau, and D. W. Holdsworth. Three-dimensional computed tomographic reconstruction using a C-arm mounted XRII: Correction of image intensifier distortion. *Med. Phys.*, 24(7), 1997.

[59] A. X. Falcão and J. K. Udupa. A 3D generalization of user-steered live-wire segmentation. *Medical Image Analysis*, 4(4):389–402, 2000.

[60] Alexandre X. Falcão et al. User-steered image segmentation paradigms: Live wire and live lane. *Graphical Models and Image Processing*, 60(4):233–260, 1998.

[61] O. D. Faugeras and M. Hebert. The representation, recognition, and locating of 3-D objects. *Int. J. Rob. Res.*, 5(3):27–52, 1986.

[62] David A. Feinberg and Alexander S. Mark. Human brain motion and cerebrospinal fluid circulation demonstrated with MR velocity imaging. *Radiology*, 163(3):793–799, 1987.

[63] Aaron Fenster and Donal B. Downey. Three dimensional ultrasound imaging. *Annual Review of Biomedical Engineering*, 2(1):457–475, 2000.

[64] Rogerio Feris, Ramesh Raskar, Kar-Han Tan, and Matthew Turk. Specular reflection reduction with multi-flash imaging. In *17'th Brazilian Symposium on Computer Graphics and Image Processing, SIBGRAPI*, pages 316–321, 2004.

[65] Gabor Fichtinger, Anton Deguet, Ken Masamune, Emese Balogh, Gregory S. Fischer, Herve Mathieu, Russell H. Taylor, S. James Zinreich, and Laura M. Fayad. Image overlay guidance for needle insertion in CT scanner. *IEEE Trans. Biomed. Eng.*, 52(8):1415–1424, 2005.

[66] Michael Figl, Christopher Ede, Johann Hummel, Felix Wanschitz, Rolf Ewers, Helmar Bergmann, and Wolfgang Birkfellner. A fully automated calibration method for an optical see-through head-mounted operating microscope with variable zoom and focus. *IEEE Trans. Med. Imag.*, 24(11):1492–1499, 2005.

[67] Gregory S. Fischer, Anton Deguet, Daniel Schlattman, Russell Taylor, Laura Fayad, S. James Zinreich, and Gabor Fichtinger. Mri image overlay: applications to arthrography needle insertion. In *Studies in Health Technologies and Informatics*, volume 119, pages 150–155, 2006.

[68] J. Michael Fitzpatrick and Jay B. West. The distribution of target registration error in rigid-body, point-based registration. *IEEE Trans. Med. Imag.*, 20(9):917–927, 2001.

[69] J. Michael Fitzpatrick, Jay Bailey West, and Clavin R. Maurer, Jr. Predicting error in rigid-body, point-based registration. *IEEE Trans. Med. Imag.*, 17(5):694–702, 1998.

[70] James D. Foley, Andries van Dam, Steven K. Feiner, and John F. Hughes. *Computer graphics (2nd ed. in C): principles and practice*. Addison-Wesley Longman Publishing Co., Inc., Boston, MA, USA, 1996.

[71] Kevin T. Foley, Yoga Raja Rampersaud, and David A. Simon. Virtual fluoroscopy: Multiplanar X-ray guidance with minimal radiation exposure. *European Spine Journal*, 8(Suppl. 1):S36, 1999.

[72] Eric M. Friets, John W. Strohbehn, John F. Hatch, and David W. Roberts. A frameless stereotaxic operating microscope for neurosurgery. *IEEE Trans. Biomed. Eng.*, 36(6):608–617, 1989.

[73] Henry Fuchs, Mark A. Livingston, Ramesh Raskar, D'nardo Colucci, Kurtis Keller, Andrei State, Jessica R. Crawford, Paul Rademacher, Samuel H. Drake, and Anthony A. Meyer. Augmented reality visualization for laparoscopic surgery. In *Medical Image Computing and Computer-Assisted Intervention*, pages 934–943, 1998.

[74] Robert L. Galloway, Jr. The process and development of image-guided procedures. *Annual Review of Biomedical Engineering*, 3:83–108, 2001.

[75] Florian Gebhard, Andreas Weidner, Ulrich C. Liener, Ulrich Stöckle, and Markus Arand. Navigation at the spine. *Injury*, 35:Suppl 1:S–A35–45, 2004.

[76] Andrew H. Gee, Richard W. Prager, Graham M. Treece, and Laurence H. Berman. Engineering a freehand 3D ultrasound system. *Pattern Recognition Letters*, 24(4-5):757–777, 2003.

[77] Isabelle M. Germano. The neurostation system for image-guided, frameless stereotaxy. *Neurosurgery*, 37(2):348–350, 1995.

[78] J. Gong, R. Bächler, M. Sati, and L. P. Nolte. Restricted surface matching, a new approach to registration in computer assisted surgery. In *Computer Vision, Virtual Reality and Robotics in Medicine and Medical Robotics and Computer-assisted Surgery*, pages 597–605, 1997.

[79] A. Ardeshir Goshtasby. *2-D and 3-D Image Registration for Medical, Remote Sensing, and Industrial Applications*. Wiley, 2005.

[80] Leo Grady, Thomas Schiwietz, Shmuel Aharon, and Rüdiger Westermann. Random walks for interactive organ segmentation in two and three dimensions: Implementation and validation. In *Medical Image Computing and Computer-Assisted Intervention*, pages 773–780, 2005.

[81] M. Grass, R. Koppe, E. Klotz, R. Proksa, M. H. Kuhn, H. Aerts, J. Op de Beek, and R. Kemkers. Three-dimensional reconstruction of high contrast objects using C-arm image intensifier projection data. *Comput. Med. Imaging Graph.*, 23(6):311–321, 1999.

[82] Michael Greenspan and Mike Yurick. Approximate K-D tree search for efficient ICP. In *International Conference on 3-D Digital Imaging and Modeling*, pages 442–448, 2003.

[83] George J. Grevera, Jayaram K. Udupa, and Dewey Odhner. An order of magnitude faster isosurface rendering in software on a PC than using dedicated, general purpose rendering hardware. *IEEE Trans. Visual. Comput. Graphics*, 6(4):335–345, 2000.

[84] W.E.L. Grimson et al. An automatic registration method for frameless stereotaxy, image guided surgery and enhanced reality visualization. *IEEE Trans. Med. Imag.*, 15(2):129–140, 1996.

[85] P. Grunert, K. Darabi, J. Espinosa, and R. Filippi. Computer-aided navigation in neurosurgery. *Neurosurg. Rev.*, 26(2):73–99, 2003.

[86] P. A. Grützner, A. Hebecker, H. Waelti, B. Vock, L. P. Nolte, and A. Wentzensen. Clinical study for registration-free 3D-navigation with the SIREMOBIL Iso-C3D mobile c-arm. *electro medica (siemens)*, 71(1), 2003.

[87] André Guéziec, Peter Kazanzides, Bill Williamson, and Russell H. Taylor. Anatomy based registration of CT-scan and intraoperative X-ray images for guiding a surgical robot. *IEEE Trans. Med. Imag.*, 17(5):715–728, 1998.

[88] Moshe Hadani, Roberto Spiegelman, Zeev Feldman, Haim Berkenstadt, and Zvi Ram. Novel, compact, intraoperative magnetic resonance imaging-guided system for conventional neurosurgical operating rooms. *Neurosurgery*, 48(4):799–809.

[89] A. Hagemann, K. Rohr, H. S. Stiehl, U. Spetzger, and J. M. Gilsbach. Biomechanical modeling of the human head for physically based, nonrigid image registration. *IEEE Trans. Med. Imag.*, 18(10):875–884, 1999.

[90] Martin Haimerl, Frank Gruenschlaeger, Andreas Oschinski, Thomas Stahelin, and Gregor Tuma. CT-fluoro based registration for minimally invasive hip surgery. In *Computer Assisted Orthopedic Surgery*, pages 147–149, 2005.

[91] Joseph. V. Hajnal, Derek L. G. Hill, and David J. Hawkes, editors. *Medical Image Registration*. CRC Press, 2001.

[92] Ali Hamadeh, Stephane Lavallée, and Philippe Cinquin. Automated 3-dimensional computed tomographic and fluoroscopic image registration. *Computer Aided Surgery*, 3(1), 1998.

[93] Thomas Hartkens, Derek L. G. Hill, Andy D. Castellano-Smith, David J. Hawkes, Calvin R. Maurer Jr., Alastair J. Martin, Walter A. Hall, Haiying Liu, and Charles L. Truwit. Measurement and analysis of brain deformation during neurosurgery. *IEEE Trans. Med. Imag.*, 22(1):82–92, 2003.

[94] Eric J. Hazan and Leo Joskowicz. Computer-assisted image-guided intramedullary nailing of femoral shaft fractures. *Techniques in Orthopaedics*, 18(2):191–200, 2003.

[95] James P. Helferty, Chao Zhang, Geoffrey McLennan, and William E. Higgins. Videoendoscopic distortion correction and its application to virtual guidance of endoscopy. *IEEE Trans. Med. Imag.*, 20(7):605–617, 2001.

[96] Jeannette L. Herring et al. Surface-based registration of CT images to physical space for image-guided surgery of the spine: A sensitivity study. *IEEE Trans. Med. Imag.*, 17(5):743–752, 1998.

[97] Derek L. G. Hill, Philipp G. Batchelor, Mark Holden, and David J. Hawkes. Medical image registration. *Phys. Med. Biol.*, 46(3):R1–R45, 2001.

[98] John H. Hipwell, Graeme P. Penney, Robert A. McLaughlin, Kawal Rohde, Paul Summers, Tim C. Cox, James V. Byrne, Alison Noble, and David J. Hawkes. Intensity-based 2D-3D registration of cerebral angiograms. *IEEE Trans. Med. Imag.*, 22(11):1417–1426, 2003.

[99] R. Hofstetter, M. Slomczykowski, M. Sati, and L. P. Nolte. Fluoroscopy as an imaging means for computer-assisted surgical navigation. *Computer Aided Surgery*, 4(2):65–76, 1999.

[100] Kathryn L. Holloway et al. Frameless stereotaxy using bone fiducial markers for deep brain stimulation. *J. Neurosurg.*, 103(3):404–413, 2005.

[101] Langston T. Holly and Kevin T. Foley. Intraoperative spinal navigation. *Spine*, 28(15S):S54–S61, 2003.

[102] B. K. P. Horn. Closed-form solution of absolute orientation using unit quaternions. *Journal of the Optical Society of America A*, 4(4):629–642, April 1987.

[103] B. K. P. Horn, H. M. Hilden, and S. Negahdaripour. Closed-form solution of absolute orientation using orthonormal matrices. *Journal of the Optical Society of America A*, 5(7):1127–1135, 1988.

[104] Jonathan S. Hott et al. Intraoperative iso-C C-arm navigation in craniospinal surgery: The first 60 cases. *Neurosurgery*, 54(5):1131–1137, 2004.

[105] Johann Hummel, Michael Figl, Christian Kollmann, Helmar Bergmann, and Wolfgang Birkfellner. Evaluation of a miniature electromagnetic position tracker. *Med. Phys.*, 29(10):2205–2212, 2002.

[106] Johann B. Hummel, Michael R. Bax, Michael L. Figl, Yan Kang, Calvin R. Maurer, Jr., Wolfgang W. Birkfellner, Helmar Bergmann, and Ramin Shahidi. Design and application of an assessment protocol for electromagnetic tracking systems. *Med. Phys.*, 32(7):2371–2379, 2005.

[107] Marcel Jackowski and Ardeshir Goshtasby. A computer-aided design system for revision of segmentation errors. In *Medical Image Computing and Computer-Assisted Intervention*, pages 717–724, 2005.

[108] Jean-Yves Jenny, Ulrich Clemens, Steffen Kohler, Hartmuth Kiefer, Werner Konermann, and Rolf K. Miehlke. Consistency of implantation of a total knee arthroplasty with a non-image-based navigation system: a case-control study of 235 cases compared with 235 conventionally implanted prostheses. *Arthroplasty*, 20(7):832–839, 2005.

[109] L. G. Johnson, P. Edwards, and D. Hawkes. Surface transparency makes stereo overlays unpredictable: the implications for augmented reality. *Stud. Health. Technol. Inform.*, 94:131–136, 2003.

[110] Ferenc A. Jolesz. Future perspectives for intraoperative MRI. *Neurosurgical Clinics of North America*, 16(1):201–213, 2005.

[111] Leo Joskowicz, Charles Milgrom, Ariel Simkin, Lana Tockus, and Ziv Yaniv. FRACAS: A system for computer-aided image-guided long bone fracture surgery. *Computer Aided Surgery*, 3(6):271–288, 1998.

[112] Timothée Jost and Heinz Hügli. A multi-resolution ICP with heuristic closest point search for fast and robust 3D registration of range images. In *International Conference on 3-D Digital Imaging and Modeling*, pages 427–433, 2003.

[113] David M. Kahler. Image guidance fluoroscopic navigation. *Clin. Orthop. Relat. Res.*, 421:70–76, 2004.

[114] W. A. Kalender, R. Hebel, and J. Ebersberger. Reduction of CT artifacts caused by metallic implants. *Radiology*, 164(2):576–577, 1987.

[115] Mannudeep K. Kalra et al. Strategies for CT radiation dose optimization. *Radiology*, 230(3):619–628, 2004.

[116] Shunichi Kaneko, Tomonori Kondo, and Atsushi Miyamoto. Robust matching of 3D contours using iterative closest point algorithm improved by M-estimation. *Pattern Recognition*, 36(9):2041–2047, 2003.

[117] Yan Kang, Klaus Engelke, and Willi A. Kalender. Interactive 3D editing tools for image segmentation. *Medical Image Analysis*, 8(1):35–46, 2004.

[118] M. Kass, A. Witkin, and D. Terzopoulos. Snakes: Active contour models. *International Journal of Computer Vision*, 1(4):321–331, 1988.

[119] Arie E. Kaufman. Volume visualization: Principles and advances. International Spring School on Visualization, Bonn, 2000.

[120] Michael R. Kaus, Jens von Berg, Jürgen Weese, Wiro Niessen, and Vladimir Pekar. Automated segmentation of the left ventricle in cardiac MRI. *Medical Image Analysis*, 8(3):245–254, 2004.

[121] Paul Keall. 4-dimensional computed tomography imaging and treatment planning. *Seminars in Radiation Oncology*, 14(1):81–90, 2004.

[122] Ali Khamene, Peter Bloch, Wolfgang Wein, Michelle Svatos, and Frank Saur. Automatic registration of portal images and volumetric CT for patient positioning in radiation therapy. *Medical Image Analysis*, 6(1):96–112, 2006.

[123] Ali Khamene, Sebastian Vogt, Fred S. Azar, Tobias Sielhorst, Frank Sauer, and Heinrich Niemann. Local 3D reconstruction and augmented reality visualization of free-hand ultrasound for needle biopsy procedures. In *Medical Image Computing and Computer-Assisted Intervention*, pages 344–355, 2003.

[124] Ron Kikinis et al. Computer assisted interactive three-dimensional planning for neurosurgical procedures. *Neurosurgery*, 38(4):640–651, 1996.

[125] Volodymyr V. Kindratenko. A survey of electromagnetic position tracker calibration techniques. *Virtual Reality: Research, Development and Applications*, 5(3):169–182, 2000.

[126] Cemil Kirbas and Francis Quek. A review of vessel extraction techniques and algorithms. *ACM Computing Surveys*, 36(2):81–121, 2004.

[127] Yasuyo Kita, Dale L. Wilson, and J. Alison Noble. Real-time registration of 3D cerebral vessels to X-ray angiograms. In *Medical Image Computing and Computer-Assisted Intervention*, pages 1125–1133, 1998.

[128] Gudrun J. Klinker, Steven Shafer, and Takeo Kanade. The measurement of highlights in color images. *International Journal of Computer Vision*, 2(1):7–32, 1988.

[129] Dotan Knaan and Leo Joskowicz. Effective intensity-based 2D/3D rigid registration between fluoroscopic X-ray and CT. In *Medical Image Computing and Computer-Assisted Intervention*, pages 351–358, 2003.

[130] E. Kobayashi et al. Quantitative evaluation of the man-machine interface for a laparoscopic manipulator system. In *Computer Assisted Radiology and Surgery*, pages 111–115, 2000.

[131] Philippe Lacroute and Marc Levoy. Fast volume rendering using a shear-warp factorization of the viewing transformation. In *SIGGRAPH*, pages 451–458, 1994.

[132] Christian Langis, Michael Greenspan, and Guy Godin. The parallel iterative closest point algorithm. In *International Conference on 3-D Digital Imaging and Modeling*, pages 195–204, 2001.

[133] David A. LaRose. *Iterative X-ray/CT Registration Using Accelerated Volume Rendering*. PhD thesis, Robotics Institute, Carnegie Mellon University, Pittsburgh, PA, May 2001.

[134] S. Lavallée. Registration for computer-integrated surgery: Methodology, state of the art. In R. H. Taylor, S. Lavallée, G. C. Burdea, and R. Mösges, editors, *Computer-integrated surgery, Technology and clinical applications*, chapter 5, pages 77–97. MIT Press, Cambridge Ma., 1996.

[135] S. Lavallée, R. Szeliski, and L. Brunie. Anatomy-based registration of three-dimensional medical images, X-ray projections, and three-dimensional models using octree-splines. In R. H. Taylor, S. Lavallée, G. C. Burdea, and R. Mösges, editors, *Computer-integrated surgery, Technology and clinical applications*, chapter 7, pages 115–143. MIT Press, Cambridge Ma., 1996.

[136] Thomas M. Lehmann, Claudia Gönner, and Klaus Spitzer. Survey: Interpolation methods in medical image processing. *IEEE Trans. Med. Imag.*, 18(11):1049–1075, 1999.

[137] L. Lemieux, R. Jagoe, D. R. Fish, N. D. Kitchen, and G. T. Thomas. A patient-to-computed-tomography image registration method based on digitally reconstructed radiographs. *Med. Phys.*, 21(11):1749–1760, 1994.

[138] Louis Lemieux, Dale L. Bailey, and David Bell. Correcting for scanner errors in CT, MRI, SPECT, and 3D ultrasound. In Joseph. V. Hajnal, Derek L. G. Hill, and David J. Hawkes, editors, *Medical Image Registration*. CRC Press, 2001.

[139] Hava Lester and Simon R. Arridge. A survey of hierarchical non-linear medical image registration. *Pattern Recognition*, 32(1):129–149, 1999.

[140] Marloes M. J. Letteboer, Peter W. A. Willems, Max A. Viergever, and Wiro J. Niessen. Brain shift estimation in image-guided neurosurgery using 3-D ultrasound. *IEEE Trans. Biomed. Eng.*, 52(2):268–276, 2005.

[141] Marc Levoy. Display of surfaces from volume data. *IEEE Comput. Graph. Appl.*, 8(3):29–37, 1988.

[142] Harel Livyatan, Ziv Yaniv, and Leo Joskowicz. Gradient-based 2D/3D rigid registration of fluoroscopic X-ray to CT. *IEEE Trans. Med. Imag.*, 22(11):1395–1406, 2003.

[143] J. Lötjönen, S. Kivistö, J. Koikkalainen, D. Smutek, and K. Lauerma. Statistical shape model of atria, ventricles and epicardium from short and long-axis MR images. *Medical Image Analysis*, 8(3):371–386, 2004.

[144] Jason P. Luck, Charles Q. Little, and William Hoff. Registration of range data using a hybrid simulated annealing and iterative closest point algorithm. In *International Conference on Robotics and Automation*, pages 3739–3744, 2000.

[145] David P. Luebke. A developer's survey of polygonal simplification algorithms. *IEEE Comput. Graph. Appl.*, 21(3):24–35, 2001.

[146] Karen E. Lunn, Keith D. Paulsen, David W. Roberts, Francis E. Kennedy, Alex Hartov, and J. D. West. Displacement estimation with co-registered ultrasound for image guided neurosrugery: A quantitative in vivo porcine study. *IEEE Trans. Med. Imag.*, 22(11):1358–1368, 2003.

[147] Burton Ma and Randy E. Ellis. Robust registration for computer-integrated orthopedic surgery: Laboratory validation and clinical experience. *Medical Image Analysis*, 7(3):237–250, 2003.

[148] Raghu Machiraju and Roni Yagel. Reconstruction error characterization and control: A sampling theory approach. *IEEE Trans. Visual. Comput. Graphics*, 2(4):364–378, 1996.

[149] Anant Madabhushi and Jayaram K. Udupa. Generalized scale: Theory,algorithms, and application to inhomogeneity correction. In *SPIE Medical Imaging: Image Processing*, pages 765–776, 2004.

[150] Andreas H. Mahnken et al. A new algorithm for metal artifact reduction in computed tomography. *Investigative Radiology*, 38(12):769–775, 2003.

[151] J. B. Antoine Maintz and Max A. Viergever. A survey of medical image registration. *Medical Image Analysis*, 2(1):1–37, 1998.

[152] B. Mansoux, L. Nigay, and J. Troccaz. The mini-screen: an innovative device for computer assisted surgery systems. *Studies in Health Technology and Informatics*, 111:314–320, 2005.

[153] Stephen R. Marschner and Richard J. Lobb. An evaluation of reconstruction filters for volume rendering. In *VIS '94: Proceedings of the conference on Visualization '94*, pages 100–107, 1994.

[154] Sandra Martelli, Simone Bignozzi, Marco Bontempi, Stefano Zaffagnini, and L. Garcia. Comparison of an optical and a mechanical navigation system. In *Medical Image Computing and Computer-Assisted Intervention*, pages 303–310, 2003.

[155] Ken Masamune, Gabor Fichtinger, Anton Deguet, Daisuke Matsuka, and Russell Taylor. An image overlay system with enhanced reality for percutaneous therapy performed inside CT scanner. In *Medical Image Computing and Computer-Assisted Intervention*, pages 77–84, 2002.

[156] Takeshi Masuda and Naokazu Yokoya. A robust method for registration and segmentation of multiple range images. *Computer Vision and Image Understanding*, 61(3):295–307, 1995.

[157] Calvin R. Maurer, Jr., Robert J. Maciunas, and J. Michael Fitzpatrick. Registration of head CT images to physical space using a weighted combination of points and surfaces. *IEEE Trans. Med. Imag.*, 17(5), 1998.

[158] Marc R. Mayberg, Eric Lapreston, and Edwin J. Cunningham. Image-guided endoscopy: description of technique and potential applications. *Neurosurg Focus. 2005 Jul 15;19(1):E10. Related Articles, Links*, 19(1):E10 (1–5), 2005.

[159] David J. Mayman, John Rudan, Jeff Yach, and Randy Ellis. The kingston periacetabular osteotomy utilizing computer enhancement: A new technique. *Computer Aided Surgery*, 7:179–186, 2002.

[160] James Mcinerney and David W. Roberts. Frameless stereotaxy of the brain. *The Mount Sinai Journal of Medicine*, 67(4):300–310, 2000.

[161] T. McInerney and D. Terzopoulos. Deformable models in medical image analysis: A survey. *Medical Image Analysis*, 1(2), 1996.

[162] Robert A. McLaughlin, John Hipwell, David J. Hawkes, J. Alison Noble, James V. Byrne, and Tim C. Cox. A comparison of a similarity-based and a feature-based 2-D3-D registration method for neurointerventional use. *IEEE Trans. Med. Imag.*, 24(8):1058–1066, 2005.

[163] Erik Meijering. A chronology of interpolation: From ancient astronomy to modern signal and image processing. *Proceedings of the IEEE*, 90(3):319–342, 2002.

[164] Michael Meissner, Jian Huang, Dirk Bartz, Klaus Mueller, and Roger Crawfis. A practical evaluation of popular volume rendering algorithms. In *VVS '00: Proceedings of the 2000 IEEE symposium on Volume visualization*, pages 81–90, New York, NY, USA, 2000. ACM Press.

[165] Ralph Metson. Image-guided sinus surgery: lessons learned from the first 1000 cases. *Otolaryngol Head Neck Surg.*, 128(1):8–13, 2003.

[166] U. Meyer et al. Evaluation of accuracy of insertion of dental implants and prosthetic treatment by computer-aided navigation in minipigs. *British Journal of Oral and Maxillofacial Surgery*, 41:102–108, 2003.

[167] Michael I. Miga, Tuhin K. Sinha, David M. Cash, Robert L. Galloway, and Robert J. Weil. Cortical surface registration for image-guided neurosurgery using laser-range scanning. *IEEE Trans. Med. Imag.*, 22(8):973–985, 2003.

[168] Steven C. Mitchell, Johan G. Bosch, Boudewijn P. F. Lelieveldt, Rob J. van der Geest, Johan H. C. Reiber, and Milan Sonka. 3-D active appearance models: Segmentation of cardiac MR and ultrasound images. *IEEE Trans. Med. Imag.*, 21(9):1167–1178, 2002.

[169] J. Montagnat, H. Delingette, and N. Ayache. A review of deformable surfaces: topology, geometry and deformation. *Image and Vision Computing*, 19(14):1023–1040, 2001.

[170] K. Mori et al. Tracking of a bronchoscope using epipolar geometry analysis and intensity-based image registration of real and virtual endoscopic images. *Medical Image Analysis*, 6:321–336, 2002.

[171] K. Mori et al. Hybrid bronchoscope tracking using a magnetic tracking sensor and image registration. In *Medical Image Computing and Computer-Assisted Intervention*, pages 543–550, 2005.

[172] Thomas M. Moriarty et al. Frameless stereotactic neurosurgery using intraoperative magnetic resonance imaging: Stereotactic brain biopsy. *Neurosurgery*, 47(5):1138–1146, 2000.

[173] Eric N. Mortensen and William A. Barrett. Interactive segmentation with intelligent scissors. *Graphical Models and Image Processing*, 60(5):349–384, 1998.

[174] Rami Mosheiff, Amal Khoury, Yoram Weil, and Meir Liebergall. First generation of fluoroscopic navigation in percutaneous pelvic surgery. *Orthopaedic Trauma*, 18(2):106–111, 2004.

[175] Rami Mosheiff, Yoram Weil, Amal Khoury, and Meir Liebergall. The use of computerized navigation in the treatment of gunshot and shrapnel injury. *Computer Aided Surgery*, 1/2:39–43, 2004.

[176] Rami Mosheiff, Yoram Weil, Eran Peleg, and Meir Liebergall. Computerised navigation for closed reduction during femoral intramedullary nailing. *Injury*, 36:866–870, 2005.

[177] Martin J. Murphy. An automatic six-degree-of-freedom registration algorithm for image-guided frameless stereotaxic radiosurgery. *Med. Phys.*, 24(6):857–866, 1997.

[178] Kazuhisa Nakada, Masahiko Nakamoto, Yoshinobu Sato, Kozo Konishi, Makoto Hashizume, and Shinichi Tamura. A rapid method for magnetic tracker calibration using a magneto-optic hybrid tracker. In *Medical Image Computing and Computer-Assisted Intervention*, pages 285–293, 2003.

[179] Shree K. Nayar, Xi-Sheng Fang, and Terrance Boult. Separation of reflection components using color and polarization. *International Journal of Computer Vision*, 21(3):163–186, 1997.

[180] Stéphane Nicolau, A. Garcia, Xavier Pennec, Luc Soler, and Nicholas Ayache. An augmented reality system to guide radio-frequency tumor ablation. *Computer Animation and Virtual Worlds*, 16(1):1–10, 2005.

[181] Stéphane Nicolau, Xavier Pennec, Luc Soler, and Nicholas Ayache. A complete augmented reality guidance system for liver punctures: First clinical evaluation. In *Medical Image Computing and Computer-Assisted Intervention*, pages 539–547, 2005.

[182] Atsushi Nishikawa et al. FAce MOUSe: A novel human machine interface for controlling the position of a laparoscope. *IEEE Trans. Robot. Automat.*, 19(5):825–841, 2003.

[183] L. P. Nolte et al. A new approach to computer-aided spine surgery: fluoroscopy-based surgical navigation. *European Spine Journal*, 9(7):78–88, 2000.

[184] Lutz P. Nolte and Reinhold Ganz, editors. *Computer Assisted Orthopaedic Surgery (CAOS)*. Hogrefe and Huber, 1999.

[185] S.D. Olabarriaga and A.W.M. Smeulders. Interaction in the segmentation of medical images: A survey. *Medical Image Analysis*, 5(2):127–142, 2001.

[186] N. Pagoulatos, R.N. Rohling, W.S. Edwards, and Y. Kim. A new spatial localizer based on fiber optics with applications in 3D ultrasound imaging. In *SPIE Medical Imaging: Image Display and Visualization*, pages 595–602, 2000.

[187] J. N. Palmer and D. W. Kennedy. Historical perspective on image-guided sinus surgery. *Otolaryngol Clin. North Am.*, 38(3):419–428, 2005.

[188] P. Parikh et al. Dynamic accuracy of an implanted wireless AC electromagnetic sensor for guided radiation therapy; implications for real-time tumor position tracking. *Med. Phys.*, 32(6):2112, 2005.

[189] Perrine Paul, Oliver Fleig, Sabine Tranchant, and Pierre Jannin. Performance evaluation of a stereoscopic based 3D surface localiser for image-guided neurosurgery. In *Medical Image Computing and Computer-Assisted Intervention*, pages 510–517, 2004.

[190] Keith D. Paulsen, Michael I. Miga, Francis E. Kennedy, Alex Hartov P. Jack Hoopes, and David W. Roberts. A computational model for tracking subsurface tissue deformation during stereotactic neurosurgery. *IEEE Trans. Biomed. Eng.*, 46(2):213–225, 1999.

[191] Vladimir I. Pavlovic, Rajeev Sharma, and Thomas S. Huang. Visual interpretation of hand gestures for human-computer interaction: A review. *IEEE Trans. Pattern Anal. Machine Intell.*, 19(7):677–695, 1997.

[192] Graeme P. Penney, Philip J. Edwards, Andrew P. King, Jane M. Blackall, Philipp G. Batchelor, and David J. Hawkes. A stochastic iterative closest point algorithm (stochastICP). In *Medical Image Computing and Computer-Assisted Intervention*, pages 762–769, 2001.

[193] Graeme P. Penney, Jürgen Weese, John A. Little, Paul Desmedt, Derek L. G. Hill, and David J. Hawkes. A comparison of similarity measures for use in 2D-3D medical image registration. *IEEE Trans. Med. Imag.*, 17(4):586–595, 1998.

[194] Terry M. Peters. Image-guided surgery: From X-rays to virtual reality. *Computer Methods in Biomechanics and Biomedical Engineering*, 4(1):27–57, 2000.

[195] Hanspeter Pfister et al. The transfer function bakeoff. *IEEE Comput. Graph. Appl.*, 21(3):16–22, 2001.

[196] Dzung L. Pham, Chenyang Xu, and Jerry L. Prince. Current methods in medical image segmentation. *Annual Review of Biomedical Engineering*, 2(1):315–337, 2000.

[197] Francis K. H. Quek. Unencumbered gestural interaction. *IEEE MultiMedia*, 3(4):36–47, 1996.

[198] M. A. Rafferty et al. Investigation of C-arm cone-beam CT-guided surgery of the frontal recess. *Laryngoscope*, 115(12):2138–2143, 2005.

[199] R. Y. Rampersaud, K. T. Foley, A. C. Shen, S. Williams, and M. Solomito. Radiation exposure to the spine surgeon during fluoroscopically assisted pedicle screw insertion. *Spine*, 25(20):2637–2645, 2000.

[200] Y. Raja Rampersaud, Justin H. T. Pik, David Salonen, and Samina Farooq. Clinical accuracy of fluoroscopic computer-assisted pedicle screw fixation: A CT analysis. *Spine*, 30(7):E183–E190, 2005.

[201] Ramesh Raskar, Kar-Han Tan, Rogerio Feris, Jingyi Yu, and Matthew Turk. Nonphotorealistic camera: depth edge detection and stylized rendering using multiflash imaging. volume 23, pages 679–688, 2004.

[202] Madan M. Rehani and Manorma Berry. Radiation doses in computed tomography. the increasing doses of radiation need to be controlled. *British Medical Journal*, 320:593–594, 2000.

[203] H. Reinhardt, H. Meyer, and E. Amrein. A computer-assisted device for the intraoperative CT-correlated localization of brain tumors. *Eur. Surg. Res.*, 20(1):51–58, 1988.

[204] H. F. Reinhardt. Neuronavigation: A ten years review. In R. H. Taylor, S. Lavallée, G. C. Burdea, and R. Mösges, editors, *Computer Integrated Surgery*, pages 329–342. MIT Press, Cambridge Ma., 1996.

[205] H. F. Reinhardt and H. J. Zweifel. Interactive sonar-operated device for stereotactic and open surgery. *Stereotact. Funct. Neurosurg.*, 54–55:393–397, 1990.

[206] Marcus Richter, Balkan Cakir, and René Schmidt. Cervical pedicle screws: Conventional versus computer-assisted placement of cannulated screws. *Spine*, 30(20):2280–2287, 2005.

[207] Martinus Richter, Jens Geerling, Stefan Zech, Michael Frink, and Christian Krettek. Iso-C-3D based computer assisted surgery (CAS) guided retrograde drilling in a osteochondritis dissecans of the talus: A case report. *Foot*, 15(2):107–113, 2005.

[208] Richard A. Robb, Dennis P. Hanson, and Jon J. Camp. Computer-aided surgery planning and rehearsal at mayo clinic. *IEEE Computer*, 29(1):39–47, 1996.

[209] David W. Roberts, Alexander Hartov, Francis E. Kennedy, Michael I. Miga, and Keith D. Paulsen. Intraoperative brain shift and deformation: A quantitative analysis of cortical displacement in 28 cases. *Neurosurgery*, 43(4):749–760, 1998.

[210] D. D. Robertson et al. Evaluation of CT techniques for reducing artifacts in the presence of metallic orthopedic implants. *Journal of Computer Assisted Tomography*, 12(2):236–241, 1988.

[211] Mitchel Robinson, Donald G. Eckhoff, Karl D. Reinig, Michelle M. Bagur, and Joel M. Bach. Variability of landmark identification in total knee arthroplasty. *Clinical Orthopaedics and Related Research*, 442:57–62, 2006.

[212] V. Rohde, P. Spangenberg, L. Mayfrank, M. Reinges, J. M. Gilsbach, and V. A. Coenen. Advanced neuronavigation in skull base tumors and vascular lesions. *Minim. Invasive Neurosurg.*, 48(1):13–18, 2005.

[213] Torsten Rohlfing et al. Reduction of metal artifacts in computed tomographies for the planning and simulation of radiation therapy. In *Computer Assisted Radiology and Surgery*, pages 57–62, 1998.

[214] Michael Rosenthal et al. A ugmented reality guidance for needle biopsies: An initial randomized, controlled trial in phantoms. *Medical Image Analysis*, 6(3):313–320, 2002.

[215] Szymon Rusinkiewicz and Marc Levoy. Efficient variants of the ICP algorithm. In *International Conference on 3D Digital Imaging and Modeling*, pages 145–152, 2001.

[216] Daniel B. Russakoff, Torsten Rohlfing, John R. Adler, Jr., and Calvin R. Maurer, Jr. Intensity-based 2D-3D spine image registration incorporating a single fiducial marker. *Academic Radiology*, 12(1):37–50, January 2005.

[217] Ofri Sadowsky, Jonathan D. Cohen, and Russell H. Taylor. Projected tetrahedra revisited: A barycentric formulation applied to digital radiograph reconstruction using higher-order attenuation functions. *IEEE Trans. Visual. Comput. Graphics*, 2006. to appear.

[218] Ibrahim A. Salama and Steven D. Schwaitzberg. Utility of a voice-activated system in minimally invasive surgery. *Journal of Laparoendoscopic and advanced surgical techniques*, 15(5):443–446, 2005.

[219] A. Schenk, G. Prause, and H. O. Peitgen. Efficient semiautomatic segmentation of 3D objects in medical images. In *Medical Image Computing and Computer-Assisted Intervention*, pages 186–195, 2000.

[220] Kurt Schicho, Michael Figl, Markus Donat, Wolfgang Birkfellner, Rudolf Seemann, Arne Wagner, Helmar Bergmann, and Rolf Ewers. Stability of miniature electromagnetic tracking systems. *Phys. Med. Biol.*, 50(9):2089–2098, 2005.

[221] Will Schroeder, Ken Martin, and Bill Lorensen. *The Visualization Toolkit, An Object-Oriented Approach To 3D Graphics*, chapter 7, pages 201–254. Kitware Inc., 2002.

[222] A. Schweikard, H. Shiomi, and J. Adler. Respiration tracking in radiosurgery without fiducials. *Int. J. Medical Robotics and Computer Assisted Surgery*, 1(2):19–27, 2005.

[223] Ramin Shahidi et al. Implementation, calibration and accuracy testing of an image-enhanced endoscopy system. *IEEE Trans. Med. Imag.*, 21(12):1524–1535, 2002.

[224] R. Sibson. Studies in the robustness of multidimensional scaling: Perturbational analysis of classical scaling. *J. Roy. Statist. Soc. B*, 41:217–229, 1979.

[225] David Simon. *Fast and Accurate Shape-Based Registration.* PhD thesis, Carnegie Mellon University, 1996.

[226] Tuhin K. Sinha, Benoit M. Dawant, Valerie Duay, David M. Cash, Robert J. Weil, Reid Carleton Thompson, Kyle D. Weaver, and Michael I. Miga. A method to track cortical surface deformations using a laser range scanner. *IEEE Trans. Med. Imag.*, 24(6):767–781, 2005.

[227] Eric P. Sipos, Scot A. Tebo, S. James Zinreich, Donlin M. Long, and Henry Brem. In vivo accuracy testing and clinical experience with the ISG viewing wand. *Neurosurgery*, 39(1):194–202, 1996.

[228] S. Skjeldal and S. Backe. Interlocking medullary nails – radiation doses in distal targeting. *Archives of Orthopaedic Trauma Surgery*, 106(3):179–181, 1987.

[229] Oskar M. Skrinjar, Colin Studholme, Arya Nabavi, and James S. Duncan. Steps toward a stereo-camera-guided biomechanical model for brain shift compensation. In *Proceedings of the 17th International Conference on Information Processing in Medical Imaging*, pages 183–189, 2001.

[230] Justin S. Smith, Alfredo Quin ones Hinojosa, Nicholas M. Barbaro, and Michael W. McDermott. Frame-based stereotactic biopsy remains an important diagnostic tool with distinct advantages over frameless stereotactic biopsy. *Neuro-Oncology*, 73(2):173–179, 2005.

[231] Kurt R. Smith, Kevin J. Frank, and Richard D. Bucholz. The neurostation^{TM} - a highly accurate, minimally invasive solution to frameless stereotactic neurosurgery. *Comput. Med. Imaging Graph.*, 18(4):247–256., 1994.

[232] M. B. Stegmann, B. K. Ersbøll, and R. Larsen. FAME - a flexible appearance modelling environment. *IEEE Trans. Med. Imag.*, 22(10):1319–1331, 2003.

[233] R. Steinmeier et al. Intraoperative magnetic resonance imaging with the magnetom open scanner: Concepts, neurosurgical indications and procedures: A preliminary report. *Neurosurgery*, 43(4):739–748, 1998.

[234] George D. Stetten and Vikram Chib. Overlaying ultrasound images on direct vision. *Journal of Ultrasound in Medicine*, 20(3):235 – 240, 2001.

[235] Martin Styner et al. Parametric estimate of intensity inhomogeneities applied to MRI. *IEEE Trans. Med. Imag.*, 19(3):153–165, 2000.

[236] Norbert Suhm, Peter Messmer, Ivan Zuna, Ludwig A. Jacob, and Pietro Regazzoni. Fluoroscopic guidance versus surgical navigation for distal locking of intramedullary implants a prospective, controlled clinical study. *Injury*, 35:567–574, 2004.

[237] Thilaka S. Sumanaweera, John R. Adler, Jr., Sandy Napel, and Gary H. Glover. Characterization of spatial distortion in magnetic resonance imaging and its implications for stereotactic surgery. *Neurosurgery*, 35(4):696–704, 1994.

[238] Hai Sun, Karen E. Lunn, Hany Farid, Ziji Wu, David W. Roberts, and Alex Hartovand Keith D. Paulsen. Stereopsis-guided brain shift compensation. *IEEE Trans. Med. Imag.*, 24(8):1039–1052, 2005.

[239] Waheeda Sureshbabu and Osama Mawlawi. PET/CT imaging artifacts. *J. Nucl. Med. Technol.*, 33(3):156–161, 2005.

[240] Jasjit S. Suri, Kecheng Liu, Laura Reden, and Swamy Laxminarayan. A review on MR vascular image processing algorithms: acquisition and prefiltering: part I. *IEEE Trans. Inform. Technol. Biomed.*, 6(4):324–337, 2002.

[241] Jasjit S. Suri, Kecheng Liu, Laura Reden, and Swamy Laxminarayan. A review on MR vascular image processing: skeleton versus nonskeleton approaches: part II. *IEEE Trans. Inform. Technol. Biomed.*, 6(4):338–350, 2002.

[242] Jasjit S. Suri, Kecheng Liu, Sameer Singh, Swamy Laxminarayan, Xiaolan Zeng, and Laura Reden. Shape recovery algorithms using level sets in 2-D/3-D medical imagery: a state-of-the-art review. *IEEE Trans. Inform. Technol. Biomed.*, 6(1):8–28, 2002.

[243] Jasjit S. Suri, Sameer Singh, and Laura Reden. Computer vision and pattern recognition techniques for 2-D and 3-D MR cerebral cortical segmentation (part I): A state-of-the-art review. *Pattern Anal. Appl.*, 5(1):46–76, 2002.

[244] Jasjit S. Suri, Sameer Singh, and Laura Reden. Fusion of region and boundary/surface-based computer vision and pattern recognition techniques for 2-D and 3-D MR cerebral cortical segmentation (part-II): A state-of-the-art review. *Pattern Anal. Appl.*, 5(1):77–98, 2002.

[245] Kar-Han Tan, James Kobler, Paul H. Dietz, Ramesh Raskar, and Rogério Schmidt Feris. Shape-enhanced surgical visualizations and medical illustrations with multi-flash imaging. In *Medical Image Computing and Computer-Assisted Intervention*, pages 438–445, 2004.

[246] Russell H. Taylor and Leo Joskowicz. Computer-integrated surgery and medical robotics. In Myer Kutz, editor, *Standard Handbook of Biomedical Engineering and Design*, chapter 29, pages 325–353. McGraw-Hill, 2002.

[247] Russell H. Taylor and Dan Stoianovici. Medical robotics in computer-integrated surgery. *IEEE Trans. Robot. Automat.*, 19(5):765–781, 2003.

[248] Scot A. Tebo, Donald A. Leopold, Donlin M. Long, S. James Zinreich, and David W. Kennedy. An optical 3D digitizer for frameless stereotactic surgery. *IEEE Comput. Graph. Appl.*, 16(1):55–64, 1996.

[249] Nicholas Theocharopoulos, Kostas Perisinakis, John Damilakis, George Papadokostakis, Alexander Hadjipavlou, and Nicholas Gourtsoyiannis. Occupational

exposure from common fluoroscopic projections used in orthopaedic surgery. *The Journal of Bone and Joint Surgery (American)*, 85:1698–1703, 2003.

[250] Dejan Tomaževič, Boštjan Likar, Tomaž Slivnik, and Franjo Pernuš. 3-D/2-D registration of CT and MR to X-ray images. *IEEE Trans. Med. Imag.*, 22(11):1407–1416, 2003.

[251] Melanie Tory, Arthur E. Kirkpatrick, M. Stella Atkins, and Torsten Möller. Visualization task performance with 2D, 3D, and combination displays. *IEEE Trans. Visual. Comput. Graphics*, 12(1):2–13, 2006.

[252] Emanuele Trucco, Andrea Fusiello, and Vito Roberto. Robust motion and correspondence of noisy 3-D point sets with missing data. *Pattern Recognition Letters*, 20(9):889–898, 1999.

[253] Greg Turk and Marc Levoy. Zippered polygon meshes from range images. In *SIGGRAPH Computer graphics and interactive techniques*, pages 311–318, 1994.

[254] Shinji Umeyama. Least-squares estimation of transformation parameters between two point patterns. *IEEE Trans. Pattern Anal. Machine Intell.*, 13(4):376–380, 1991.

[255] Everine B. van de Kraats, Bart Carelsen, Wytske J. Fokkens, Sjirk N. Boon, Niels Noordhoek, Wiro J. Niessen, and Theo van Walsum. Direct navigation on 3D rotational x-ray data acquired with a mobile propeller C-arm: accuracy and application in functional endoscopic sinus surgery. *Phys. Med. Biol.*, 50(24):5769–5781, 2005.

[256] Everine B. van de Kraats, Graeme P. Penney, Dejan Tomaževič, Theo van Walsum, and Wiro J. Niessen. Standardized evaluation methodology for 2-D3-D registration. *IEEE Trans. Med. Imag.*, 24:1177–1189, 2005.

[257] Bram van Ginneken, Mikkel B. Stegmann, and Marco Loog. Segmentation of anatomical structures in chest radiographs using supervised methods: a comparative study on a public database. *Medical Image Analysis*, 10(1):19–40, 2006.

[258] B. C. Vemuri, J. Ye, Y. Chen, and C. M. Leonard. Image registration via level-set motion: Applications to atlas-based segmentation. *Medical Image Analysis*, 7(1):1–20, 2003.

[259] Kris Verstreken et al. An image-guided planning system for endosseous oral implants. *IEEE Trans. Med. Imag.*, 17(5):842–852, 1998.

[260] Jan Victor and Davy Hoste. Image-based computer-assisted total knee arthroplasty leads to lower variability in coronal alignment. *Clinical Orthopaedics and Related Research*, 428:131–139, 2004.

[261] Alan T. Villavicencio, Sigita Burneikiene, Ketan R. Bulsara, and Jeffrey J. Thramann. Utility of computerized isocentric fluoroscopy for minimally invasive spinal surgical techniques. *J. Spinal Disord. Tech.*, 18(4):369–375, 2005.

[262] H. Visarius, J. Gong, C. Scheer, S. Haralamb, and L. P. Nolte. Man-machine interfaces in computer assisted surgery. *Computer Aided Surgery*, 2(2):102–107, 1997.

[263] Deming Wang, Wendy Strugnell, Gary Cowin, David M. Doddrell, and Richard Slaughter. Geometric distortion in clinical MRI systems part I: evaluation using a 3D phantom. *Magn. Reson. Imaging*, 22(9):1211–1221, 2004.

[264] Deming Wang, Wendy Strugnell, Gary Cowin, David M. Doddrell, and Richard Slaughter. Geometric distortion in clinical MRI systems part II: correction using a 3D phantom. *Magn. Reson. Imaging*, 22(9):1223–1232, 2004.

[265] Simon K. Warfield et al. Advanced nonrigid registration algorithms for image fusion. In Arthur W. Toga and John C. Mazziotta, editors, *Brain Mapping: The Methods, Second Edition*. Academic Press, 2002.

[266] Simon K. Warfield et al. Capturing intraoperative deformations: research experience at Brigham and Women's hospital. *Medical Image Analysis*, 9:145–162, 2005.

[267] Stefan Weber, Martin Klein, Andreas Hein, T. Krueger, Tim Lüth, and Jürgen Bier. The navigated image viewer - evaluation in maxillofacial surgery. In *Medical Image Computing and Computer-Assisted Intervention*, pages 762–769, 2003.

[268] Greg Welch and Eric Foxlin. Motion tracking: No silver bullet, but a respectable arsenal. *IEEE Comput. Graph. Appl.*, 22(6):24–38, 2002.

[269] W. M. Wells et al. Adaptive segmentation of MRI data. *IEEE Trans. Med. Imag.*, 15(4):429–442, 1996.

[270] Jay West et al. Comparison and evaluation of retrospective intermodality brain image registration techniques. *Journal of Computer Assisted Tomography*, 4(4):554–568, 1997.

[271] Jay B. West and Calvin R. Maurer, Jr. Designing optically tracked instruments for image-guided surgery. *IEEE Trans. Med. Imag.*, 23(5):533–545, 2004.

[272] Anders Westermark, Stefan Zachow, and Barry L. Eppley. Three-dimensional osteotomy planning in maxillofacial surgery including soft tissue prediction. *Journal of Craniofacial Surgery*, 16(1):100–104, 2005.

[273] Lee Westover. Footprint evaluation for volume rendering. In *SIGGRAPH*, pages 367–376, 1990.

[274] Karl Heinz Widmer and Paul Alfred Grützner. Joint replacement-total hip replacement with CT-based navigation. *Injury*, 35(1):S–A84S–A89, 2004.

[275] Marcin Wierzbicki, Maria Drangova, Gerard Guiraudon, and Terry Peters. Validation of dynamic heart models obtained using non-linear registration for virtual reality training, planning, and guidance of minimally invasive cardiac surgeries. *Medical Image Analysis*, 8(3):387–401, 2004.

[276] S. Wirth et al. C-arm based computed tomography - a comparative study. In *Computer Assisted Radiology and Surgery*, pages 408–413, 2001.

[277] S. K. Wise and J. M. DelGaudio. Computer-aided surgery of the paranasal sinuses and skull base. *Expert Rev Med Devices*, 2(4):395–408, 2005.

[278] Anthony B. Wolbarst and William R. Hendee. Evolving and experimental technologies in medical imaging. *Radiology*, 238(1):16–39, 2006.

[279] Lawrence B. Wolff and Terrance E. Boult. Constraining object features using a polarization reflectance model. *IEEE Trans. Pattern Anal. Machine Intell.*, 13(7):635–657, 1991.

[280] Xiaohui Wu and Russell Taylor. A direction space interpolation technique for calibration of electromagnetic surgical navigation systems. In *Medical Image Computing and Computer-Assisted Intervention*, pages 215–222, 2003.

[281] Ying Wu and Thomas S. Huang. Vision-based gesture recognition: A review. In *Gesture Workshop*, volume 1739 of *LNCS*, pages 103–115. Springer, 1999.

[282] Roni Yagel and Arie E. Kaufman. Template-based volume viewing. *Comput. Graph. Forum*, 11(3):153–167, 1992.

[283] Pingkun Yan and Ashraf A. Kassim. MRA image segmentation with capillary active contour. In *Medical Image Computing and Computer-Assisted Intervention*, pages 51–58, 2005.

[284] Ziv Yaniv, Leo Joskowicz, Ariel Simkin, Maria Garza-Jinich, and Charles Milgrom. Fluoroscopic image processing for computer-aided orthopaedic surgery. In *Medical Image Computing and Computer-Assisted Intervention*, pages 325–334, 1998.

[285] L. J. Zamorano, L. P. Nolte, A. M. Kadi, and Z. Jiang. Interactive intraoperative localization using an infrared-based system. *Stereotact Funct Neurosurg*, 63(1–4):84–88, 1994.

[286] L. Zhang et al. Accuracy and precision of implantable radiofrequency transponder localization measurements conducted using multislice CT. *Med. Phys.*, 32(6):2106, 2005.

[287] Zhengyou Zhang. Iterative point matching for registration of free-form curves and surfaces. *International Journal of Computer Vision*, 13(2):119–152, 1994.

[288] Barbara Zitová and Jan Flusser. Image registration methods: a survey. *Image and Vision Computing*, 21(11):977–1000, 2003.

[289] Lilla Zöllei, W. Eric L. Grimson, A. Norbash, and William M. Wells III. 2D-3D rigid registration of X-ray fluoroscopy and CT images using mutual information and sparsely sampled histogram estimators. In *Proc. of IEEE Computer Vision and Pattern Recognition Conf.*, 2001.